University of Alberta

The Role of Autotaxin in the Regulation of Lysophosphatidylcholine-Induced Cell Migration

by

Cristoforo Giuseppe Gaetano

A thesis submitted to the Faculty of Graduate Studies and Research
in the partial fulfillment of the requirements for the degree of

Master of Science

Department of Biochemistry

Spring 2010
Edmonton, Alberta

EXAMINING COMMITTEE

Dr. David N Brindley, Biochemistry, University of Alberta

Dr. Charles F Holmes, Biochemistry, University of Alberta

Dr. Marek Michalak, Biochemistry, University of Alberta

Dr. Todd McMullen, Medicine (Division of Surgery), University of Alberta

TO MY PARENTS

ABSTRACT

Increased expression of autotaxin has been shown to promote metastasis formation and cancer proliferation. These actions could be related to the catalytic activity of autotaxin which converts lysophosphatidylcholine into lysophosphatidate extracellularly or non-catalytic functions of autotaxin may be responsible. Also both LPC and LPA have been reported to stimulate migration through their respective receptors. This work investigates the role of autotaxin in controlling the motility of two cancer cell lines. With the use of autotaxin inhibitors we were able to block LPC-induced migration. Knocking-down autotaxin secretion also blocked stimulation of migration by LPC. Autotaxin inhibitors abolished any migratory effects from media collected from autotaxin secreting cells. We determined that LPC alone is unable to stimulate migration. Also we did not observe non-catalytic effects of autotaxin on migration. This thesis provides strong evidence that the inhibition of autotaxin production or activity would provide a beneficial therapy in the prevention of tumour growth or metastasis in patients with autotaxin expressing tumours.

ACKNOWLEDGEMENTS

I would like to express my gratitude to:

Dr. David Brindley
For your consistent guidance and encouragement.

Dr. Charles Holmes, Dr. Marek Michalak, and Dr. Todd McMullen
For your advice and support.

The Brindley Lab members: Jay, Nasser, Carlos, Katherine, Anja, Chif, Meltem, Bern, Vitali and others.

Members of the Biochemistry Department and the Signal Transduction Research Group.

Everyone who supported me throughout my study.

TABLE OF CONTENTS

LIST OF FIGURES

LIST OF ABBREVIATIONS

ADP	adenosine diphosphate
Akt	serine-threonine protein kinase B
ATP	adenosine triphosphate
ATX	autotaxin
BMP2	Bone morphogenetic protein-2
BSA	bovine serum albumin
cAMP	cyclic adenosine monophosphate
Cdc42	cell division cycle 42/GTP-binding protein
CNS	central nervous system
DAG	diacylglycerol
DMSO	dimethyl sulfoxide
EDG	endothelial differentiation gene
EDTA	ethylenediaminetetraacetic acid
ERK	extracellular signal-regulated kinase
FBS	fetal bovine serum
FBS-C	charcoal-stripped fetal bovine serum
FGF	Fibroblast growth factor
FS-3	fluorogenic substrate-3
G2A	G_2 accumulation
GAPDH	glyceraldehyde 3-phosphate dehydrogenase
GEF	guanine nucleotide exchange factor

GPR	G-protein-coupled receptor
GSK3β	glycogen synthase kinase 3β
GTP	guanosine triphosphate
HBS	HEPES buffered saline
IgG	immunoglobulin G
IL	Interleukin
INF	Interferon
IP_3	inositol triphosphate
JNK	c-jun amino-terminal kinase
kDA	kilodaltons
LCAT	lecithin/cholesterol acyltransferase
LPA	lysophosphatidate/lysophosphatidic acid
LPC	lysophosphatidylcholine
LPP	lipid phosphate phosphatase
LysoPLD	lysophospholipase D
MAPK	mitogen-activated protein kinase
MEK	mitogen-activated protein kinase kinase
MLC II	myosin light chain II
MORFO	modulator of oligodendrocyte remodeling and focal adhesion organization
mRNA	messenger ribonucleic acid
NF-κB	nuclear factor κB
NH-LPA	non-hydrolysable lysophosphatidate
NMDA	N-methyl-d-asparate

NPP	nucleotide pyrophosphate and phosphodiesterase
PA	phosphatidate/phosphatidic acid
PBS	phosphate buffered saline
PI3K	phosphoinositol 3-kinase
PKA	protein kinase A
PKC	protein kinase C
PLB	phospholipase B
PLD	phospholipase D
PPAR	peroxisome proliferators-activating receptor
Rac1	ras-related C3 botulinum toxin substrate 1
rATX	recombinant autotaxin
RNA	ribonucleic acid
ROCK	Rho-associated kinase
RT-PCR	reverse transcriptase polymerase chain reaction
S1P	sphingosine-1-phosphate
SDS-PAGE	sodium dodecyl sulphate polyacrylamide gel electrophoresis
siATX	small interfering ATX RNA
SPC	sphingosylphosphorylcholine
$sPLA_2$	secretory phospholipase A2
TGF	tumour growth factor
VEGF	vascular endothelial growth factor
VEGFR	vascular endothelial growth factor receptor
Wnt-1	Wingless-type MMTV integration site family, member 1

CHAPTER 1

INTRODUCTION

1.1 Overview of Cancer

Cancer today remains one of the leading causes of death worldwide; over the last 20 years science has made several advancements in cancer treatment and for the first time we have begun to see a steady decline in cancer related deaths. As we better understand the mechanisms that lead to the development and progression of aggressive malignancies, the better suited we are to provide life saving or prolonging strategies to deal with this devastating disease. While we have made great strides in the management of primary tumours, we still struggle greatly in the treatment of metastatic lesions at sites distant to the primary tumour [1]. In determining cancer patient outcomes, the two factors that suggest a poor prognosis are most often the involvement of lymph nodes and presence of metastasis, the latter being the cause of the majority of cancer related deaths [2]. Metastasis depends upon the ability of cancer cells to migrate, break tissue barriers, and invade surrounding tissue. However, much of how this process occurs is still poorly understood [3]. In order for cells to acquire the ability to metastasize, there are often several alterations that must occur within the cell such as increased growth potential, loss of apoptotic safe guards, detachment from the extracellular matrix, migration and invasion of tissue barriers; this along with changes to the tumor microenvironment allow for the progression of cancer [4]. In fact, it is believed that changes in the tumour microenvironment are as important to the advancement of cancer as are changes within the cells themselves [5]. The affected organ and the invading cells produce factors in the microenvironment that alter tumour growth, tumour survival, blood vessel

formation, and cell migration [6]. One of these factors, the secreted enzyme, autotaxin (ATX), has received much attention in recent years as a strong modifier of the extracellular environment.

1.2 History of Autotaxin

Autotaxin is a 125-kDa glycoprotein that was first identified as a motility-stimulating factor purified from human melanoma A2058 cells. When it was first identified, the enzymatic activity was not known, and no homology to any other growth or motility factors were identified, but it was shown to stimulate migration through a G-protein coupled receptor [7]. Later it was found to have significant homology to the nucleotide pyrophosphatase and phosphodiesterase (NPP) family [8]. These are transmembrane enzymes that hydrolyze phosphodiester and pyrophosphate bonds that remove phosphates from ATP and ADP [9]. ATX was described as an excreted NPP and was shown to exhibit 5′-nucleotide phosphodiesterase activity, thus it was co-named NPP2 [10]. Ten years after its initial discovery a more important function of ATX was identified. Extracellular lysophospholipase D (lysoPLD) activity was demonstrated in rat plasma that generates lysophosphatidic acid (LPA) from lysophosphatidylcholine (LPC) [11]. Upon further analysis the secreted lysoPLD was shown to be identical to ATX [12]. ATX is activated first by cleavage of a 27-residue signal peptide by signal peptidase followed by the cleavage of 8-residue peptide by pro-protein convertase [13]. Both the phosphodiesterase and lysoPLD activity of ATX rely on the same critical residue, specifically threonine 210 in the catalytic domain, and the reaction mechanisms are similar (FIG 1.1A). However, it is now believed that the

majority of the physiological actions of ATX are mediated through the lysoPLD activity and not through its action on nucleotide phosphates [14].

1.3 Autotaxin and Cancer

In addition to melanoma, ATX has been associated with several other malignancies [15-21]. Elevating ATX expression in Ras-transformed NIH3T3 cells enhanced their invasive, metastatic and tumourigenic properties [22]. Increased expression of ATX has been shown to contribute to tumour growth, inhibition of apoptosis, migration, invasion, and metastasis [12, 18, 22-24]. ATX may also contribute to tumour growth by promoting angiogenesis [24]. Vascular endothelial growth factor (VEGF)-A promotes expression of ATX and ATX is able to promote the expression of VEGF receptor (VEGFR)-1 and -2 suggesting that ATX and VEGF act in a positive-feedback loop [25]. Higher levels of ATX activity have been linked to worse prognosis in patients with ovarian and thyroid carcinomas [20, 21]. The association of malignancy and ATX has been vigorously investigated in recent years but ATX is also associated with many other physiological and pathological actions.

1.4 Physiological Actions of Autotaxin

There are several identified biological functions of ATX; failure on several attempts to produce live ATX null mice is a testament to its necessity in normal physiology. ATX has an identified role in the stabilization of blood vessels which is most likely why ATX knockout mice die early in embryonic

development with significant vascular abnormalities [26, 27]. ATX mRNA is found in most tissues in the body, with highest expression in brain, ovary, lung, intestine and kidney [28]. The myelination of axons by oligodendrocytes is in part controlled by the action of ATX [29]. ATX is detectable in blister fluid at high concentrations and may be involved in reepithelialization by keratinocytes [30]. ATX is involved in the regulation of thrombosis where it binds with activated platelets localizing LPA production [31]. ATX has a role in innate and adaptive immunity [32]. It promotes the recruitment of immune cells in the presence of bacterial lipopolysaccharide during the inflammatory response [33]. ATX is also implicated several pathological conditions other than cancer. High levels of ATX can be found in affected joints of rheumatoid arthritis patients and may be a contributing factor in joint destruction. ATX induces synoviocytes to produce potent neutrophil attracting cytokines [34]. Involvement of ATX causing the proliferation of preadipocytes suggests a role for it in the development of obesity [35]. Also ATX is believed to be involved in the progression of inflammatory bowel disease, neuropathic pain and Hepatitis C [36-38]. At the beginning of this work the role of ATX in the mechanisms behind these actions was not fully understood, there has been some work on non-catalytic effects of ATX, however many of the physiological and pathological functions are now believed to be related to the lysoPLD activity of ATX [28].

Essentially, there are three differentially expressed isoforms of ATX (FIG 1.1B). ATX β mRNA is highly expressed in peripheral tissues and poorly expressed in the CNS, conversely ATX γ mRNA is expressed primarily in the

CNS with low expression in the periphery [39]. Besides their distinctive localizations the β and γ isoforms have very similar biochemical characteristics [40]. ATX α mRNA is poorly expressed in all tissues and the protein is unstable due to an extra exon not found in β or γ isoforms, the extra exon encodes a protease cleavage site (KVAPKRR) corresponding to amino acid 341 (FIG 1.1B). Cleavage at this site is within the catalytic domain of ATX, thus the α isoform lacks enzymatic activity [40].

1.5 Non-Catalytic Functions of Autotaxin

Non-catalytic effects of ATX have been identified in oligodendrocytes where it effects remodeling and focal adhesion organization as a matrixcellular protein [41]. This function is mediated through the *M*odulator of *O*ligodendrocyte *R*emodeling and *F*ocal adhesion *O*rganization (MORFO) domain located at the C-terminal end of the protein (FIG 1.1A) [14]. The MORFO domain is able to prevent the adhesion of oligodendrocytes to the extracellular matrix and thus may effect cell migration and myelination by oligodendrocytes in the early stages of CNS development [42]. This domain was shown to function independently of the lysoPLD activity and mutations in the C-terminal region did not impair lysoPLD activity or the ability of ATX to stimulate cell motility [43].

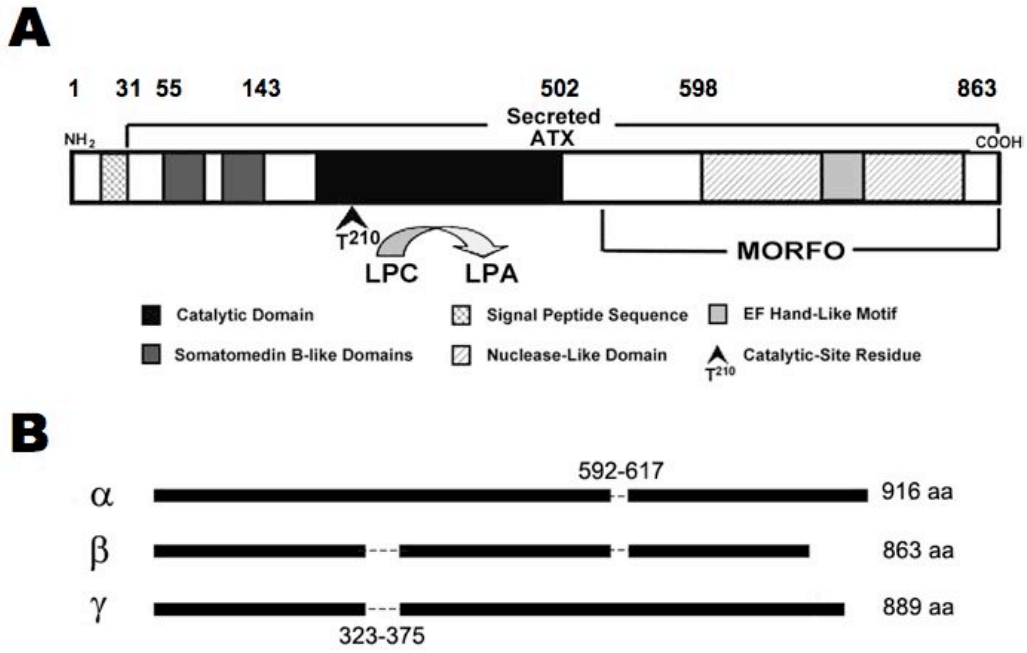

FIGURE 1.1: Schematic of autotaxin domains and alternatively spliced autotaxin transcripts. *Panel A* represents a schematic of autotaxin identifying the different structure-functional domains; threonine 210 is a critical residue for the lysophospholipase D activity of autotaxin. Adapted from Yuelling and Fuss, 2008. *Panel B* represents mRNA splice variants in the structure of murine autotaxin. In the α and β variants, exon 20 is spliced directly to exon 22, whereas in the β and γ variants exon 11 is spliced directly to exon 13. The addition of exon 12 in the α variant encodes for a protease cleavage site that makes the α isoforms unstable. Adapted from Giganti *et al.,* 2008 [40].

1.6 Autotaxin Activity and LPA production

As mentioned ATX was first identified as a 5′-phosphodiesterase due to its NPP structural homology, but in comparison to the other members of the NPP family, ATX was found to be only a weak phosphodiesterase with nucleotide phosphates [44]. Instead the lysoPLD activity is much more potent, and ATX was shown to have a much higher affinity for LPC than for standard phosphodiesterase substrates [45]. ATX is also able to hydrolyze sphingosylphosphorylcholine (SPC) into sphingosine-1-phosphate (S1P) [46]. Like LPA, S1P is a potent phospholipid with several biological actions such as; mobilization of intracellular Ca^{2+}, actin stress fiber formation, stimulation of endothelial cell migration, angiogenesis and maintenance of cell growth [47]. S1P is also an immune modulator that promotes T cell differentiation, migration and cytokine production [48]. However the production of S1P by ATX *in vivo* is in question. This is mainly because the K_m value of ATX for SPC is higher than the levels found in plasma and the concentration of LPC in plasma is three orders higher than that of SPC. Therefore, it is unlikely ATX is the source of most of the extracellular S1P [28]. ATX is a constitutively active enzyme and LPC is in great supply in plasma at concentrations as high as 200 μM [49]. So many questions are raised to how ATX activity is regulated and of the circulating levels of LPA in the plasma are maintained. One mechanism for the regulation of ATX is through the end products LPA and S1P, which act in a negative feedback manner and inhibit ATX activity [50]. The affinity of ATX for both of these lipids is much higher that that of LPC. Therefore, even with the high concentrations of LPC in

the blood small concentrations of LPA or S1P are able to restrict further LPA production by ATX [50]. The intimate relationship between LPA levels and ATX is further demonstrated in mice with heterozygous ATX knockdown ($atx^{+/-}$), where these mice were shown to have about half the plasma LPA levels as control mice [27].

There are several pathw0ays proposed for the production of extracellular LPA, but besides the ATX pathway only one other is considered physiologically relevant. This involves the production of LPA through the action of secretory phospholipase A2 ($sPLA_2$) which deacylates phosphatidic acid (PA) at the *sn*-2 position (FIG 1.2). This would occur during an inflammatory response with membranes that have lost there normal phospholipid asymmetry, thus exposing PA to the extracellular environment [51, 52]. However it is now believed that the primary source of LPA is from hydrolysis of LPC through the lysoPLD activity of ATX [28], which cleaves the phosphodiester bond between choline and phosphate (FIG 1.2).

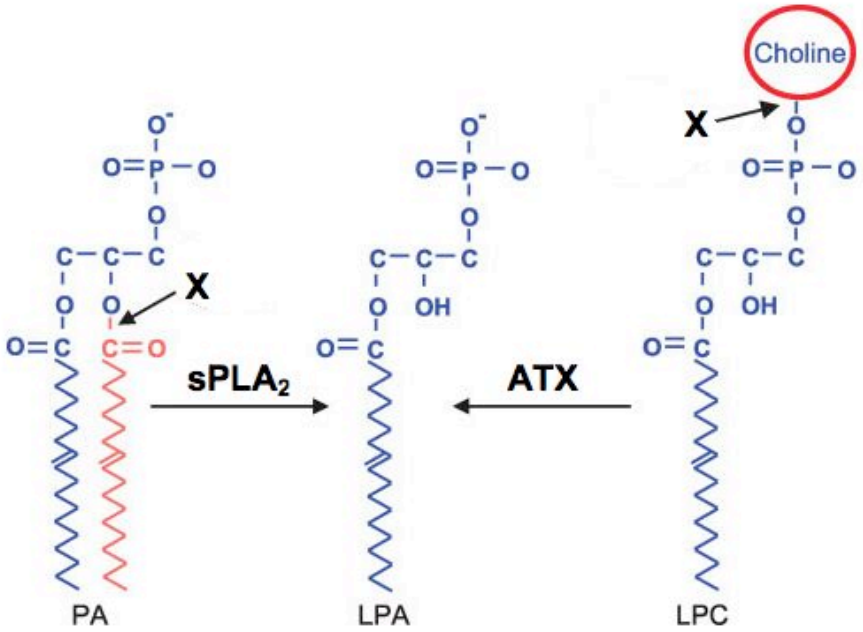

FIGURE 1.2: Lysophosphatidic acid production by autotaxin and phospholipase A2. LPA can be produced through the degradation of LPC by ATX or by the hydrolysis of PA by PLA_2. The sites of cleavage are represented by an X. Figure from Moolenaar, Meeteren and Giepmans, 2004 [53].

1.7 Biological Activities of LPC and Receptor Controversy

LPC is the primary substrate for ATX, it is an abundant extracellular lipid that is found in the circulation at high concentrations [49]. There are two main pathways for the production of LPC. The liver produces and secretes mainly polyunsaturated LPC [49]. Alternatively in plasma, a mainly saturated form is produced from high-density lipoproteins through the action of lecithin/cholesterol acyltransferase (LCAT) [54]. There are other LCAT independent sources of LPC through the actions of phospholipase A_1 and A_2 related enzymes, but they do not appear to be significant contributors to circulating LPC concentrations [55]. Pathological conditions such as diabetes and atherosclerosis have been linked to high levels of LPC [56].

Several papers have suggested that LPC can act as an extracellular ligand and activate G-protein-coupled receptor-4 (GPR4) and G2A (G_2 accumulation) receptors and this is able to stimulate cell signaling and cell migration [57-61]. However, more recent investigations have identified GPR4 and G2A purely as proton-sensing receptors that are activated by changes in pH and are instead antagonized by LPC [55, 62]. Also, much of the work describing LPC as a ligand for these receptors has been retracted [63]. However, there still may be a role for LPC, not as a direct ligand, but instead as a regulator of G2A receptor mobilization to the cell membrane [64]. Much of this is still controversial and continued research needs to be done to determine a definitive role for LPC in cell signaling. Many of the previously identified functions of LPC are now thought to be due to the actions of ATX and LPA production.

1.8 Physiological and Pathological Effects of LPA

Lysophosphatidic acid (mono-acylglycerol-3-phosphate) is a potent cell-signaling molecule; it consists of a single acyl-chain at *sn*-1 or *sn*-2 position and a phosphate head group on a glycerol backbone (FIG 1.3). Aside from its relatively simple structure LPA has a multitude of biological actions that include cell proliferation, protection from apoptosis, wound healing, neurite retraction and cell migration [28, 47]. LPA has also been implicated in the promotion of several malignancies, which will be discussed in greater detail further on. LPA is associated with platelet activation and it is contained in mildly oxidized low density lipoproteins suggesting a possible roles in thrombosis and arthrosclerosis [65]. Proliferation of pre-adipocytes was stimulated by LPA suggesting it has a function in the regulation of adipogenesis [35]. Both the physiological and pathological process associated with LPA are mediated by signaling though several G-protein-coupled receptors.

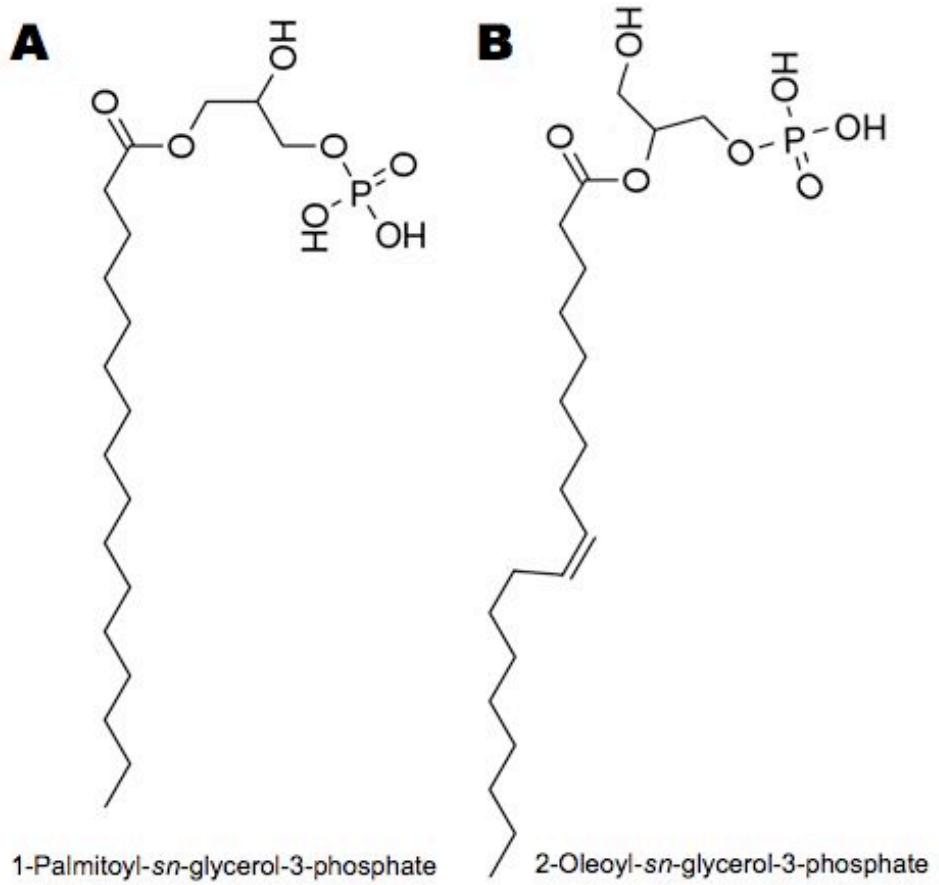

FIGURE 1.3: Structures of the most common lysophosphatidic acid isoforms. Lysophosphatidic acid most common structures (A) with palmitate (16:0) in the sn-1 position, or (B) with oleoyl (18:1) in the sn-2 position, this position is also often occupied by linoleoyl (18:2).

1.9 LPA Receptors

Seven LPA cell surface receptors have been identified to date: LPA_1/EDG2, LPA_2/EDG4, LPA_3/EDG7, LPA_4/GPR23/p2y9, LPA_5/GPR92, LPA_6/p2y5 and GPR87 [66-70]. LPA_{1-3} have a ubiquitous distribution and belong to the endothelial differentiation gene (EDG) receptor subgroup that includes five other S1P-activated G-protein coupled receptors [71]. The other four receptors belong to the P2Y subgroup and they have specific tissue distributions. LPA_4/GPR23/p2y9 is abundantly expressed in ovarian tissue and LPA_5/GPR92 is most abundant in small intestine and dorsal root ganglion cells [71]. LPA_6/p2y5 is found in inner root sheaths of hair follicles and contributes to hair growth [55]. GPR87 is highly expressed in testes and brain but also found in the placenta, ovaries, prostate and skeletal muscle [70]. They transduce different responses by coupling to different sets of G proteins [55]. Activations of the various G-proteins instigate a multitude of effects that are depicted in FIGURE 1.4. For example, the activation of $G_{i/o}$ causes a decrease in cAMP and induces Ras-Raf-ERK pathway and also activates phosphoinositol 3-kinase (PI3K) and Rac pathways promoting cell proliferation, survival and migration (FIG 1.4). The Ras-Ref-ERK pathway is shown to be involved in the activation of phospholipase D2 (PLD2) resulting in PA production at the cell membrane and integrin formation [72]. Activation of $G_{12/13}$ affects cytoskeletal elements that effect cell morphology, stress fiber formation and extracellular matrix interactions through Rho and Cdc42 (FIG 1.4). The activation of G_q causes the activation of phospholipase C which then produces diacylglycerol (DAG) and inositol

triphosphate (IP_3) that causes Ca^{2+} mobilization from the endoplasmic reticulum (FIG 1.4). Signaling by DAG and Ca^{2+} activates the classic protein kinase C (PKC) isoforms and DAG alone activates the novel PKCs [73]. Activation of PKCs through G_q and Rho activation via $G_{12/13}$ increases phospholipase D1 (PLD1) activation resulting in the production of PA [73]. Finally, G_s activation causes adenylate cyclase activation and subsequent cAMP production that activates protein kinase A (FIG 1.4).

In addition to its role in extracellular signaling, LPA has a proposed function as an intracellular messenger by activating nuclear receptors. The LPA_1 receptor can be translocated to the nucleus, where upon LPA binding, it is able to regulate gene transcription of proteins involved in inflammation such as cyclooxygenase-2 and inducible nitric oxide synthase [74]. There is also evidence that LPA can bind to peroxisome proliferators-activating receptor γ (PPARγ) and induce transcription of genes involved in vascular remodeling and neointima formation [75], a process that can lead to atherosclerotic disease. However another study showed that activation of LPA_1 decreases PPARγ in adipocytes which contradicts the previous findings [76]. Hence the relationship between LPA and PPARγ is still unclear. Overall, LPA is a key regulator in cell physiology, which is exemplified by the number of receptors and pathways it can activate.

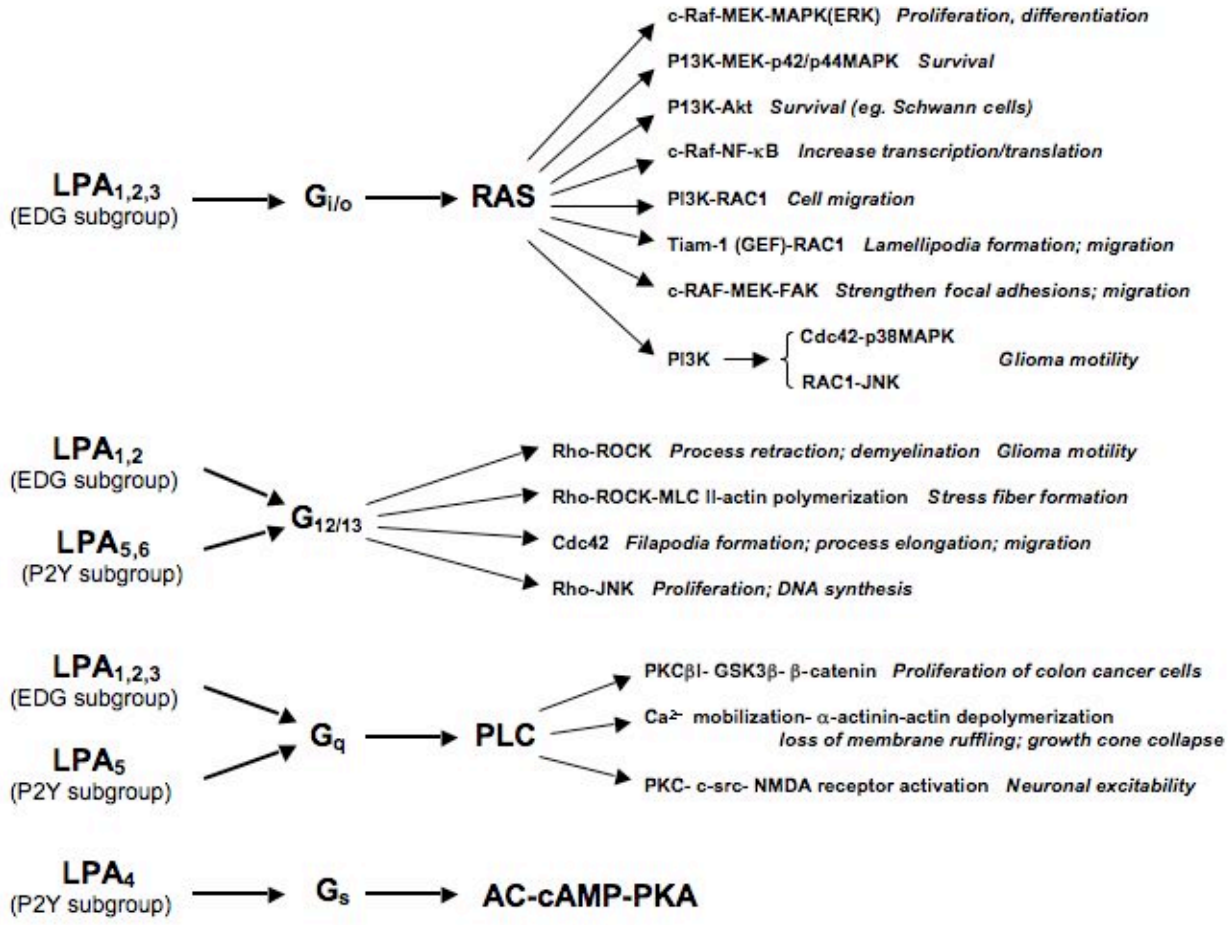

FIGURE 1.4: Major signaling pathways activated by LPA receptors. Shown are several examples of intercellular pathways activated by LPA receptors. The activation of different LPA receptors when coupled with various G-proteins can effect several cell functions which are shown in italics. Figure from Gardell *et al.,* 2006 [77].

1.10 LPA and Cell Migration

Most relevant to this work is the ability of LPA to induce cell migration. LPA has been shown to stimulate cell migration in several mammalian cell types [78]. Cell movement in response to LPA can occur via two mechanisms; chemokinesis or chemotaxis [78-81]. Chemokinesis is the random non-directed movement of a cell in response to a stimulus; chemotaxis involves directed cell movement towards a concentration gradient for a given chemoattractant. The migratory response is dependent on the activation of specific cell-surface LPA receptors. For most cancer cell lines migration is stimulated through activation of LPA_1 and activation of LPA_2 often has an inhibitory effect [82, 83]. There are exceptions, for instance, the migration of SCOV3 and HEY ovarian cancer cells requires the activation of LPA_2 and LPA_3 receptors [84]. The specific LPA receptor that is involved in migration varies greatly between cell types and depends on the G-proteins to which they are coupled. However, migration is induced through receptor activation of $G_{i/o}$ and $G_{12/13}$ followed by activation of three Rho GTPases, RhoA, Rac, and Cdc42 [85]. These work in concert by polarizing the cell and reorganizing the cytoskeletal elements and focal adhesions to facilitate cell movement (FIG 1.5). Rac and Cdc42 are both found primarily at the leading edge of the cell, Cdc42 is believed to define cell polarity and regulate the direction of movement [86]. Activation of Rac stimulates actin polymerization causing cell membrane ruffling and protrusion, it also assists in the formation of focal adhesions at the front of the cell [85]. RhoA regulates the assembly of actin:myosin contractile elements resulting in contraction a the rear

of the cell body and it also required for the disassembly of cell adhesions at the trailing edge of the cell [86, 87].

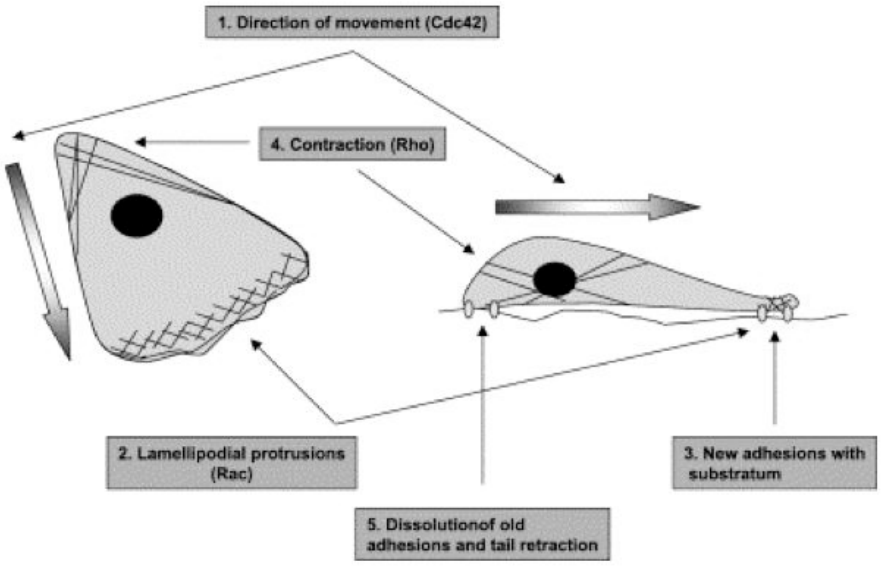

FIGURE 1.5: A migrating cell (seen from the top and side). A migrating cell needs to perform a coordinated series of steps to move. Cdc42 regulates the direction of migration, Rac induces membrane protrusion at the front of the cell through stimulation of actin polymerization and integrin adhesion complexes, and Rho promotes actin:myosin contraction in the cell body and at the rear. From Raftopoulou and Hall, 2004 [86].

1.11 Turnover of Extracellular LPA

Most cells will exhibit a maximum migratory response at a specific LPA concentration, and they will be less responsive to concentrations above and below this amount. Therefore the enzymes that control the production and degradation of LPA are important in regulating the actions of LPA. The degradation of extracellular LPA is mediated by the action of three lipid phosphate phosphatases (LPPs) [88]. LPPs are integral membrane proteins that regulate several functions in cell signaling; they function as ecto-enzymes at the plasma membrane and on the luminal side of Golgi membranes and endoplasmic reticulum [89]. LPPs are able to hydrolyze LPA into mono-acylglycerol and a phosphate and also hydrolyze other lipid phosphates such as PA, S1P, ceramide-1-phosphate and diacylglycerol pyrophosphate[89].

Overexpression of LPPs has been shown to attenuate cell growth, survival, division and cancer tumourigenesis in various cell lines [88]. Overexpression of LPP-3 in ovarian cancer decreased colony formation in these cells and this finding was reversed with a non-hydrolysable LPA analog [90]. As well increased LPP-1 expression in ovarian cancer cells showed increased LPA hydrolysis, resulting in decreased proliferation and increased apoptosis [91]. Increased LPP-1 activity in platelets was able to prevent LPA-induced platelet aggregation and LPA accumulation and proliferation of preadipocytes is regulated by LPPs [92, 93]. These LPP related actions are in opposition to the actions of LPA suggesting that LPPs may reverse the effects of ATX. Interestingly, LPP-1 overexpressing mice showed no differences in circulating LPA levels, which may be due to increased production of LPA via ATX [94]. However in mouse models with decreased LPP-1 expression, the plasma LPA concentrations were significantly higher [95].

LPP-1 depleted mice had a significantly extended half-life of plasma LPA to ~12 min compared to a half-life of 3 min in control animals. This strongly supports a role for LPP-1 in regulating circulating LPA levels and turnover.

The LPPs are also able to regulate several cellular function though regulation of intracellular phospholipid concentrations. LPPs are able to breakdown PA to produce DAG, thus decreasing PA concentrations while increasing DAG concentrations, both of which have roles in intracellular signaling [88]. However, given that LPP activity is extracellular or on the luminal surface, PA must be efficiently transported across cell membranes in order for this to occur [96]. Our group showed that increased LPP-1 expression decreased LPA-induced migration in fibroblasts but did not effect migration by platelet-derived growth factor. The effect on LPA-induced migration was also shown to be independent of extracellular LPA hydrolysis, with the use of a non-hydrolysable LPA analog [79]. Significantly, activation of PLD2, but not PLD1, was necessary for LPA-induced fibroblast migration. An increased LPP-1 expression can inhibit LPA-induced migration by blocking PA accumulation upstream of PLD activation [79]. Similar results were found with S1P-induced migration where PLD activation was downstream of PA and PKC-ε activation but upstream of PKC-ζ activation [97].

Furthermore, LPPs are implicated in the regulation of LPA release by cells [98]. For example, LPA release from activates platelets was increased with the addition of a specific LPP-1 inhibitor [92]. Collectively the degradation of extracellular LPA, the decrease of LPA production, and the effects downstream of LPA receptor activation, suggest an important role for LPPs in the regulation of the biological actions of LPA.

1.12 Regulation of Autotaxin and Inhibition of Activity

Another way to regulate LPA actions is to control the production and activity of ATX. Circulating ATX has a rapid turnover and expression is stimulated by several growth factors, such as EGF, FGF, BMP2 and Wnt-1, and inhibited by TGFβ, IL-1, IL-4 and INF-γ [53, 99]. One could use agonists and antagonists to the respective receptors for these cell modulators to control ATX levels, although this may not be practical due to the numerous other biological functions these growth factors and cytokines have. A more direct method is through the use of ATX inhibitors. Several inhibitors have been produced and studied in recent years. Cyclic phosphatidic acid, an analog of LPA, inhibits ATX activity but does not activate LPA receptors and it was shown to inhibit invasion and metastasis in melanoma cells in vivo [100]. Specific small-molecule inhibitors that were developed against ATX decreased migration and invasion in melanoma cells [101]. Our lab was able to show that ATX activity protects MDA-MB-435 and MCF-7 cells against Taxol-induced apoptosis. Subsequently, with the addition of VPC8a202 or S32826, two ATX inhibitors, we were able to disrupt protection against apoptosis by ATX [102]. Alpha-bromophosphonate-LPA, a pan-LPA receptor antagonist and ATX inhibitor, significantly reduced tumour growth in mice [103]. These findings strongly support the possible use of ATX inhibitors in cancer chemotherapy.

1.13 Roles of LPA and LPA Receptors in Malignancy

Due to its several migratory and cell supportive actions aberrant LPA signaling has been also been associated with the development and progression of malignancies. The association of LPA and carcinogenesis was first made when it was shown to be an activating factor in ovarian cancer that promoted cell proliferation and metastasis [104]. The ascites fluid of ovarian tumours were shown to contain high concentrations of LPA [105]. LPA reduced the abundance of p53 tumour suppressor in A549 lung carcinoma cells [106]. LPA increases the expression of urokinase plasminogen activator, matrix metalloproteinases and cyclooxygenase-2 in ovarian cancer cells, all of which promote increased invasiveness [107-109]. Most of the tumour promoting actions are mediated through LPA_{1-3} receptors. Stimulation of LPA_1 increases the motility and metastatic potential of several cancer cell lines [81, 110]. Increased LPA_2 or LPA_3 expression was shown to increase the ovarian cancer aggressiveness [111]. Knockdown of LPA_2 was shown to decrease invasion of endometrial cancer and significantly reduce colon cancer growth in animal models [112, 113]. LPA_2 was found to be overexpressed in patients with invasive ductal breast carcinoma [114]. LPA can also promote tumour growth by stimulating angiogenesis by elevating levels of VEGF [23]. The synthesis of macrophage inhibitory factor, a tumour promoter, is increased by LPA in a colon cancer cell line [115]. A recent study has shown that overexpression of ATX or the LPA receptors, LPA_{1-3}, individually in transgenic mice cause an increase in mammary carcinomas and metastasis

[116]. These findings strongly suggest a therapeutic potential in regulating the levels of LPA and the stimulation of LPA receptors in the treatment of cancer.

1.14 Thesis Objectives

Much of the tumour and metastasis promoting actions of LPA parallel those found with ATX. In order to further understand the role of the ATX-LPA axis in the role of metastasis we worked some common cancer cell lines. MDA-MB-231 cells are derived from a primary breast tumour of stromal origin with strong invasive and metastatic potential [117]. MDA-MB-435 cells we originally isolated as a breast cancer cell line but the current consensus is they are, in fact, melanoma cells [118]. Similarly, MDA-MB-435 cells are known to be highly invasive and metastatic and they are even more aggressive than the MDA-MB-231 cell line [117]. MCF-7 cells are a commonly used breast cancer cell line that are of epithelial cell origin. These cells are estrogen receptor positive, weakly invasive and usually require estrogenic stimulation for tumourigenesis [117]. The differences in ATX expression at the protein and mRNA levels in these cells were used to help us prove our hypothesis.

Autotaxin is now believed to be the primary source of extracellular LPA. Both ATX and LPA have been associated with several physiological and pathological actions. The importance of the ATX-LPA axis in cancer growth, survival, invasion and metastasis has been of particular interest in recent years. In this thesis, we examined the effect of LPC and LPA on the migration of some common cancer cell lines. We used MDA-MB-435 melanoma cells that secrete

abundant amounts of ATX and they were compared to MDA-MB-231 and MCF-7 cells that do not express significant amounts of ATX. Several experiments were conducted using these cell lines and the changes in the properties of the media that are produced during their incubations. We hypothesized that: 1) LPC could stimulate migration directly thorough its putative receptors; and 2) ATX could stimulate migration through LPA production or through its non-catalytic effects on cell adhesion. Due to the numerous cancer-promoting effects of ATX, we also proposed that the production of ATX by MDA-MB-435 cells promotes a tumourigenic environment. The aim of this work was, therefore, to investigate the necessity of ATX activity in LPC induced migration. To do this, we used some newly developed ATX inhibitors and tested their efficacy with a recently developed ATX assay. We also used siRNA knockdown of ATX in MDA-MB-435 cells and $LPA_{1/3}$ antagonist to determine the effects of ATX-induced LPA production.

The elucidation of the role of ATX in migration will prove useful in the fight against cancer. Given that there is an abundance of LPC in extracellular environment the role of ATX needs to be clarified to determine if it is a potential target for decreasing tumour growth and metastasis.

CHAPTER 2

MATERIALS AND METHODS

2.1 Materials

VPC8a202 was a gift from Drs. K.R. Lynch and T.L. Macdonald (Department of Pharmacology, University of Virginia Health System Charlottesville, VA). VPC32183 was purchased from Avanti Polar Lipids (Alabaster, AL). FS-3 compound (fluorogenic LysoPLD/Autotaxin substrate) was purchased from Echelon Biosciences (Salt Lake City, UT). Recombinant ATX protein and rabbit polyclonal ATX antibody were gifts from Dr. Tim Clair (National Cancer Institute, Bethesda, MA). S32826 was a gift from Dr. Jean Boutin (Institut de Recherches Servier, Croissy-sur-Seine, France). Reagents used were of the highest grade available. Lysophosphatidylcholine (oleyol) and Lysophosphatidate (oleyol) were purchased from Sigma Chemical Co. (St. Louis, MO).

2.2 Growth and Maintenance of Cell Lines

MDA-MB-435, MDA-MB-231, and MCF-7 breast cancer cells were obtained from the American Type Culture Collection (ATCC). The cells were maintained in RPMI 1640 medium (GIBCO) supplemented with 10% (v/v) fetal bovine serum (FBS) (Medicorp Inc., Montreal, PQ, Canada) and an antibiotic/antimycotic (A/A) cocktail (penicillin, streptomycin, amphoterecin B from Invitrogen Life Technologies, Carlsbad CA) at 5% CO_2, 95% humidity, and 37 °C. Cells were passaged once they reached 80-90% confluency; cells were washed with 37 °C HEPES buffered saline (HBS) and trypsinized with trypsin-EDTA and generally were split 1:10. In order to preserve cell lines, flasks at approximately 80% confluency were trypsinized, collected in growth media,

centrifuged, and the pellet was re-suspended in 4 °C RPMI 1640 with 10% FBS and 5% DMSO. Cells were then frozen and stored in liquid nitrogen.

2.3 Extraction of Proteins

Dishes were placed on ice and cells were washed with ice-cold HBS twice and then scraped in lysis buffer and collected. Lysis buffer contained 50mM HEPES, 137mM NaCl, 1mM $MgCl_2$, 1mM $CaCl_2$, 10% (v/v) glycerol, 0.1% (v/v) SDS, 1% (v/v) Triton X-100, 0.5% (v/v) sodium deoxycholate, and 2.5mM EDTA. Protein concentration of the samples was determined using a BCA™ assay (Bio-Rad) according to the manufacturer's instructions, using duplicate samples placed in a 96 well plate. Absorbance of sample and standard solutions was measured using an EAR 340AT (SLT Lab instruments) spectrophotometer.

2.4 Collection and Concentration of Conditioned Media

Equal numbers of cells were plated onto 10 cm dishes and grown until they reached 90% confluence. One dish of cells was selected for trypsinization and counting, other dishes were washed twice with HBS and then 10 mL of RPMI 1640 containing 0.1% BSA (≥96% fatty acid free), with or without treatment, was added to each flask. After 24 h cells were washed twice with HBS and 10mL of plain RPMI 1640 was added to each dish. Dishes were incubated again for 24 h, with or without additional treatment, the media were collected and cells on each dish were counted. Collected media were then spun at 1500 x g for 10 min to remove any whole cells or debris and stored at -20 °C. Media were concentrated

approximately 20- to 30-fold using Centricon® YM-10 centrifugal filter devices (Millipore). Filters were pre-rinsed with 2 ml of water to remove glycerine and samples were centrifuged at 5000 x g for 120 min or until the final desired volume was reached. Filters were then inverted and centrifuged at 1500 x g for 2 min to collect concentrated conditioned media. The final volume was determined by weighing.

2.5 mRNA Expression

Total RNA was extracted from cell lysates using the RNAqueous kit, according the manufacture's instruction. DNA-free kit was also applied to remove contaminating DNA from RNA preparation. Total RNA was reverse-transcribed using superscript II reverse transcriptase (Invitrogen; Carlsbad, CA) in the presence of a random hexamer primer. As a control, a minus reverse transcriptase reaction was performed in parallel to ensure the absence of genomic DNA contamination. cDNA was calculated assuming 100% conversion from RNA. For real time-RT-PCR, 25 μL of master mix containing 2 × Syber Green buffer mix and forward and reverse primers (Invitrogen), were added to 3.5 μL of sample in 96 well plates. As an internal control a 316 bp fragment of the constitutively expressed housekeeping human glyceraldehyde 3-phospate dehydrogenase (GAPDH) was used. Primers for human ATX were: sense, 5′-ACAACGAGGAGAGCTGCAAT-3′, and anti-sense, 5′-AGAAGTCCAGGCTGGTGAGA-3′. Primers for human GAPDH were: sense, 5′-ACAGTCAGCCGCATCTTCTT-3′ and antisense, 5′-

GACAAGCTTCCCGTTCTCAG-3´. Samples of standard cDNA and sample cDNA were run in triplicates on the 7500 Real Time PCR System (Applied Biosystems). The transcript number of human GAPDH was quantified, and each sample was normalized on the basis of GAPDH mRNA content.

2.6 Knockdown of Autotaxin Expression using siRNA

Knockdown of ATX was achieved using *SMARTpool*® small interfering RNAs (siRNAs) (Dharmacon Inc., Lafayette CO). The siRNAs consist of four duplex siRNAs designed to target separate sequences on human ATX transcript (hENPP2). Transfection efficiency and the optimum Lipofectamine™ 2000 (Invitrogen) concentration was determined using siGLO® (Dharmacon). Three concentrations of Lipofectamine™ 2000 were tested; low, medium, and high (5, 10, and 20 µL of Lipofectamine™ per mL of medium). At high Lipofectamine™ concentrations there appeared to be a significant loss of viable cells (19.8% apoptotic cells, 96.8% transfection efficiency) and at low concentration the transfection efficiency was poor (9.8% apoptotic cells, 48.6% transfection efficiency). Therefore a medium Lipofectamine™ concentration was determined to be the optimal for siATX transfection (12.4% apoptotic cells, 95.2% transfection efficiency) (FIG 2.1). About 800,000 cells were plated on 10 cm dishes with 15 mL of antibiotic-free RPMI 1640 containing 10% FBS cells were allowed to grow for two days (reaching approx 50% confluency). Three hours before transfection, old media was replaced with 7 mL of fresh antibiotic-free media. Ten µL of stock siRNA (50µM) was diluted in 1.5 mL of Opti-MEM Reduced Serum Medium (Invitrogen). In a separate tube 30 µL of

Lipofectamine™ 2000 was mixed with 1.5 mL Opti-MEM and incubated at room temperature for 15 min. The siRNA and the Lipofectamine™ 2000 solutions were then combined and incubated for another 15 min at room temperature. Each dish of cells received 3 mL of the siRNA-Lipofectamine™ 2000 complex that was added drop wise while swirling the dish. Final concentrations of Lipofectamine™ 2000 and siRNA were 1.4 μg/mL and 50 nM respectively. Cells were incubated for 24 h at 37ºC and then used to collect conditioned media by the procedure described above. Following collection of conditioned media, cells on each dish were trypsinized and counted in order to standardize conditioned media concentrations.

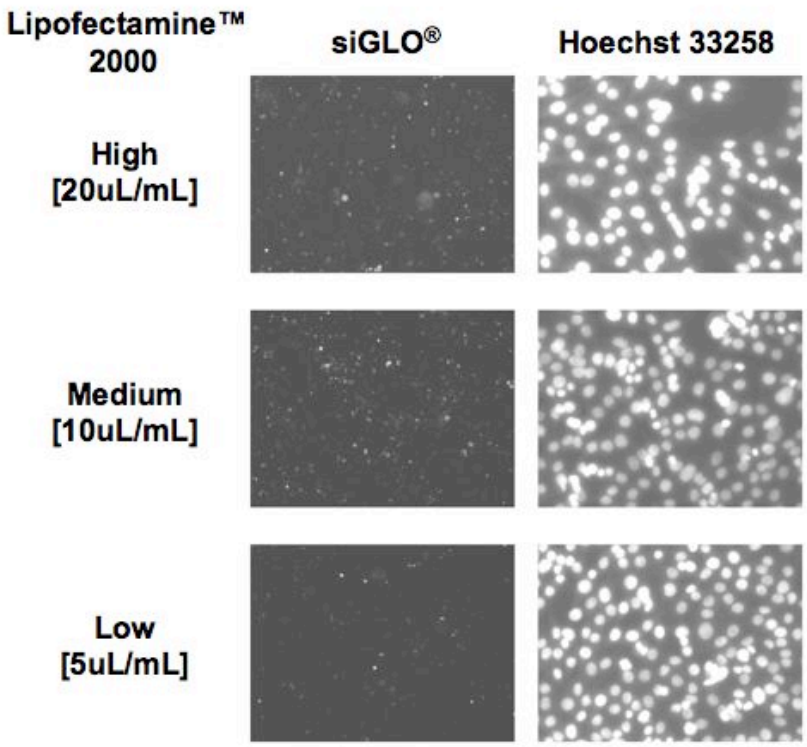

FIGURE 2.1: Optimization of siRNA transfection efficiency using siGLO®. MDA-MB-435 cells were transfected with siGLO® fluorescent siRNAs using 3 different concentration of Lipofectamine™ 2000. Cells were stained with Hoechst 33258 for 1-2 h prior to imaging. Images for siGLO® incorporation and Hoechst were obtained by viewing with an excitation wavelength of 495 nm and 365 nm respectively. Panels depict typical cells from several fields. Results displayed are from one experiment.

2.7 Boyden Chamber Assay for Migration

Two million cells were seeded in a 25 cm^2 flask with growth medium for at least 48 h. Prior to migration cells were then starved with starvation media, RPMI 1640 containing 0.1% BSA (≥96% fatty acid free), for the last 18 hrs. The day before migration Transwells® (polycarbonate, 13mm D, 12 μm pore size, Corning, Corning, NY) were coated with 120 μL of 0.15 mg/ml fibronectin and allowed to dry in a cell culture hood. Cells were washed twice with HBS, trypsinized, and collected in starvation medium and 1 mL of 0.1% trypsin inhibitor solution in HBS. Cells were spun down, the media were removed by aspiration, and cells were resuspended in starvation medium. 300,000 cells were seeded into each of the fibronectin coated Transwell® filters and incubated for 45 min for attachment. Filters were then transferred into bottom chambers that contained 1.5 mL of starvation medium with 0.2% charcoal-treated FBS (FBS-C) and various agonists. This charcoal treatment removed >95% of the LPA as assessed after spiking the FBS with ^{32}P-labeled LPA determined in previous work in our lab. Five % FBS was used as a positive control, whereas starvation medium and 0.2% FBS-C was used to measure basal migration levels. Chambers were incubated at 37 °C and cells were allowed to migrate through the pores in the filter for 3 or 6 h with the agonist in the bottom chamber. After migration cells were then fixed in 5% formaldehyde for 1 h, or overnight. Filters were then rinsed in water and place in 1 μg/mL Hoechst 33258 stain for 2 h. Cells were then observed under fluorescent microscope to insure uniform distribution of cells across the filter, then top side of filers were cleaned with a moist cotton swab to

remove cells that had not migrated. Filters were washed again and place in PBS. Four to six random fields were photographed under the fluorescent microscope at 100 X magnification, and numbers of cells per field were counted without knowing the treatments. Results were averaged and counts were expressed as a percentage relative to the basal migration rate for each experiment.

2.8 SDS-PAGE and Protein Transfer

Concentrated conditioned media and cell lysate samples were dissolved in sample loading buffer (0.25 M Tris base, pH 6.8, 13% glycerol, 2.5% SDS, 0.1mg/mL bromophenol blue) with 5% β-mercaptoethanol added. Samples were heated to 100 °C for 5 min and then allowed to cool to room temperature before loading. Samples were separated by electrophoresis at 120 volts at 4 °C for approximately 1.5 h using PAGE and Laemmli electrophoresis buffer (0.19 M Glycine, 0.025 M Tris base, 0.1% SDS). Stacking gels were composed of 3.9% acrylamide, 0.1% bisacrylamide, 0.375 M Tris-HCl pH 6.8, and 0.1% SDS. ATX was resolved with 10% acrylamide/ 0.27% bisacrylamide, 0.125 M Tris-HCl, pH 8.8, and 0.1% SDS separating gels. Molecular mass markers (Precision Plus Protein™ Standards, All Blue, Bio-Rad) were loaded onto each gel and gels were developed in Laemmli electrophoresis buffer (0.19 M glycine, 0.025 M Tris base, 0.1% SDS) at 120 volts at 4 °C for approximately 1.5 h. Proteins were transferred at 450 mA for 5 h onto 0.45 μm pure nitrocellulose membrane (Trans-Blot® Transfer Medium, Bio-Rad) in transfer buffer (192 mM glycine, 24 mM Tris base, and 20% (v/v) ethanol).

2.9 Antibodies and Imaging

Membranes were blocked in 50% PBS and 50% Odyssey™ blocking buffer (Li-Cor Biosciences, Lincon, NE) for a minimum of 1.5 h, or overnight. All antibodies were diluted in 50/50 PBS/Odyssey™ blocking buffer with 0.1% (v/v) Tween 20. Membranes were first incubated with primary antibody at room temperature for 1 h, washed 4 times for 15 min with wash buffer (PBS with 0.1% Tween 20), then incubated in fluorescent-conjugated secondary antibody for 1 h and washed 3 times for 15 min in wash buffer and 1 time in PBS alone. Membranes were incubated, washed, and stored in the dark until scanning. Primary antibodies used were: anti-GAPDH (mouse, 1:5000, Sigma); anti-ATX (rabbit, 1:10,000). Secondary antibodies were: AlexaFluor© 680 goat anti-mouse IgG, A-21057 (Invitrogen, 1:10,000) and IRDye 800 goat anti-rabbit IgG (Rockland Immunochemicals, Philadelphia, PA, 1:10,000). Membranes were scanned using the Odyssey™ Imager (Li-Cor). Anti-rabbit IgG was scanned at 800 nm and appeared as green on the screen; anti-mouse IgG was scanned at 700 nm and appeared as red. Images were converted to black and white by Odyssey™ software for figures.

2.10 LysoPLD/Autotaxin Activity Assay

To determine autotaxin activity, we developed an assay based on the method described by Fergurson et al., 2006 [119]. A fluorogenic phospholipid LysoPLD/autotaxin substrate, FS-3, was used (Echelon Biosciences, Salt Lake City, UT). FS-3 is a LPC analog where a fluor quencher (dabscyl) is attached to the *sn*-1 acyl chain position and a hydrophilic fluor (fluorescein) is attached to the

phosphate in the head group position. ATX hydrolyzes the phosphodiester bond of the substrate releasing the fluorescent head group causing a measurable increase in fluorescence (FIG 2.2C). FS-3 was diluted to a concentration of 3.125 µM in a solution containing: 140 mM NaCl, 5 mM KCl, 1mM $CaCl_2$, 1mM $MgCl_2$, 50 mM Tris/ HCl, pH 8.0, and 1 mg/ml BSA. The solution was heated at 60 ºC for 10 min and then cooled to 37 °C before use. Forty µl of FS-3 solution was added to 10 µl of cell lysate or concentrated conditioned media in a black 96 well Costar® half-area plate. Measurements were then taken at regular intervals using Fluoroskan Ascent fluorometer (Thermo Lab Systems) at an excitation wavelength of 485 nm and an emission wavelength of 527 nm. In order to test the assay, the increase in fluorescence was measured over a 12 h period using two amounts of recombinant ATX (67 ng and 134 ng). Within a reasonable experimental error the response in fluorescence over time was proportional to the amount of ATX present in the first 90 min. For further experiments, determination of relative activity was obtained using only the linear portion of the curve that occurred between 0 to 90 min (FIG 2.2A,B).

2.11 Statistics

Results were presented as means ± SEM from at least 3 independent experiments, unless otherwise indicated. Statistical differences were calculated using GraphPad 4 software (Prism) by ANOVA with a Newman-Keuls post-hoc test and Paired T-tests were performed between two samples.

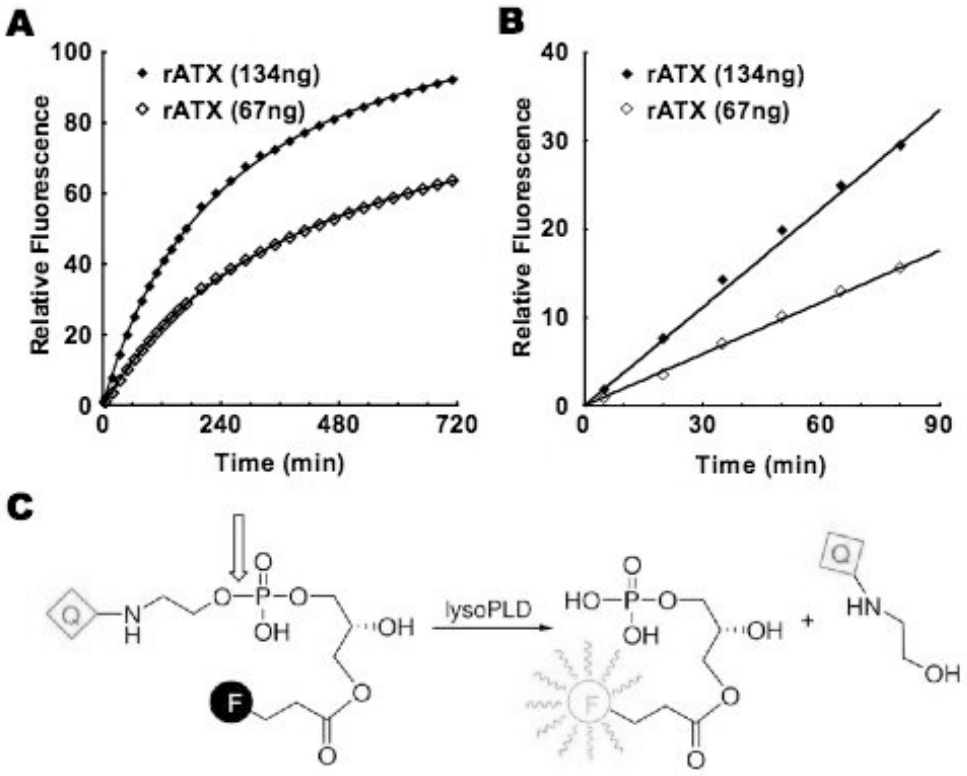

FIGURE 2.2: Determination of the linear range for the ATX activity fluorescence assay. Panel A shows the results from a 12 h fluorescence assay for ATX activity of 134 ng (◆) and 67 ng (◇) of recombinant ATX. Panel B shows the first 90 minutes of the same assay illustrating where the curve is most linear. Results are from one experiment. Panel C illustrates the release of the fluorescence head group from its quencher on FS-3 when hydrolyzed by ATX/lysoPLD. Panel C obtained from Ferguson *et al*., 2006 [119].

CHAPTER 3

RESULTS

3.1 Differential Effects of LPC and LPA on the Migration of MDA-MB-231 Breast Cancer Cells and MDA-MB-435 Melanoma Cells

Our interest in this work first arose due to the identification of some major differences in the characteristics of commonly studied cancer cells lines. Initially we conducted various migration experiments with 3 cancer cell lines: MDA-MB-231 and MCF-7 breast cancer cells and MDA-MB-435 cells. MDA-MB-435 cells were previously identified to be breast cancer cells but now have been determined to be derived from M14 melanoma cells [118]. We attempted to stimulate migration of the cancer cell lines by adding charcoal-treated FBS and various concentrations of LPA to the bottom wells in our Boyden chambers and allowed the cells to migrate over a 3 h incubation. Our MCF7 cells failed to migrate with any concentration of LPA tested or 5% FBS, a result which is compatible with previous work [120], suggesting that these cells are migration deficient without alteration. On the other hand, MDA-MB-231 and MDA-MB-435 migrated well in the presence of LPA. Also, both cell lines exhibited similar responses to differing LPA concentrations with maximal migration occurring with 0.5 μM LPA. This LPA concentration elicited a migratory response similar to that obtained with 5% FBS, which was used as a positive control for both cell lines (FIG 3.1). We also examined the migration of MDA-MB-231 and MDA-MB-435 cells with stimulation by various concentrations of LPC. MDA-MB-231 cells showed no significant stimulation of migration over the 6 h incubation with any concentration of LPC. By contrast, MDA-MB-435 cells showed significant migration when 5 μM and 10 μM LPC concentrations were added (FIG 3.2).

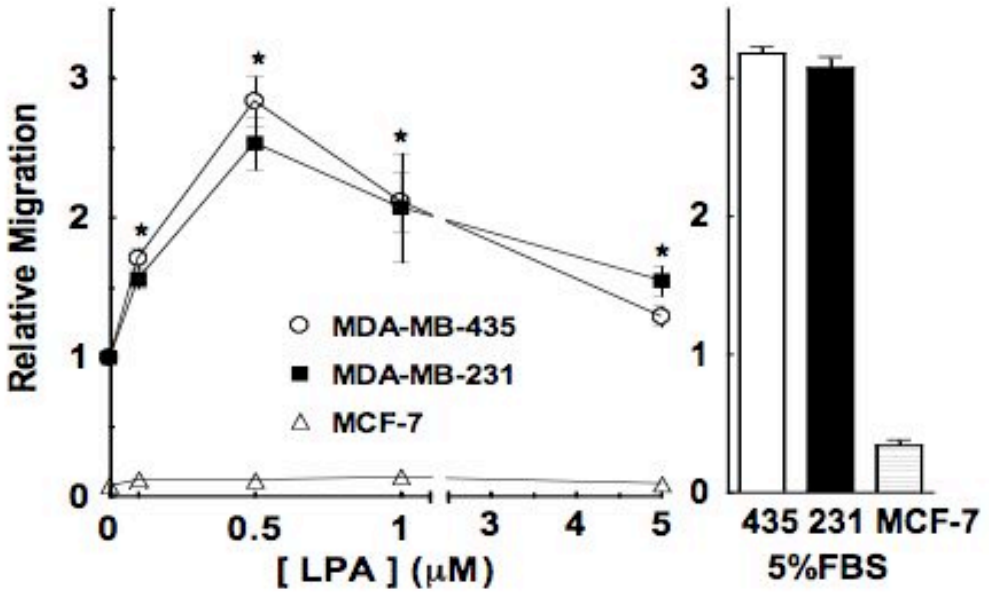

FIGURE 3.1: Effects of LPA on the migration of MDA-MB-435, MDA-MB-231, and MCF-7 cells. The migration of MDA-MB-435 (○), MDA-MB-231 (■), and MCF-7 (△) cells is shown after a 3 h incubation with different concentrations of LPA in the bottom chamber. Migration in response to 5% charcoal-stripped FBS (FBS-C) was used as a positive control. The results are expressed relative to the number of cells migrating with only basal media (RPMI 1640 with 0.1% BSA and 0.2% FBS-C), which is given a value of 1. Typically, migration with basal media resulted in approximately 75 cells per field over a 3 h incubation for both MDA-MB-435 and MDA-MB-231 cells, an average of only 7 cells per field were observed for MCF-7 cells and they are represented relative to the 2 other cell lines. Results are means ± SEM from at least 3 independent experiments. Statistically significant differences between basal migration and agonist are indicated by * ($p < 0.01$).

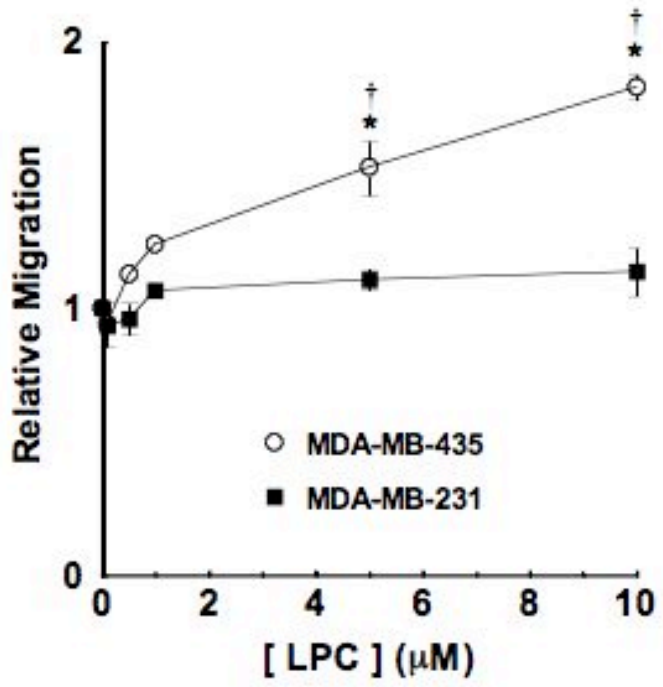

FIGURE 3.2: Effects of LPC on the migration of MDA-MB-435 and MDA-MB-231 cells. The migration of MDA-MB-435 (○), and MDA-MB-231 (■) cells is shown after a 6 h incubation with different concentrations of LPC. The results are expressed relative to the number of cells migrating with only basal media (RPMI 1640 with 0.1% BSA and 0.2% FBS-C), which is given a value of 1. Typically, migration with basal media resulted in approximately 120 cells per field for a 6 h incubation. Results are means ± SEM from at least 3 independent experiments. Statistically significant differences between basal migration and agonist are indicated by * ($p < 0.01$) and between cell lines are indicated by † ($p < 0.01$).

3.2 Addition of Phospholipase B Abolishes Migration of MDA-MB-231 and MDA-MB-435 Cells in the Presence of LPA

In order to show that the stimulation of migration in FIGURE 3.1 was dependent upon the addition of LPA we examined the migration of MDA-MB-231 and MDA-MB-435 cells using LPA, a non-hydrolysable analog of LPA (NH-LPA) and phospholipase B (PLB). Phospholipase B is able to hydrolyze the ester linkages of the acyl chains from both the sn-1 and sn-2 positions of phospholipids, thus it will destroy any surrounding LPA or LPC in the migration media. On the other hand, the acyl group on the non-hydrolysable analog is attached by an ether linkage and cannot be cleaved by PLB. The addition of phospholipase B (PLB) abolished the strong migratory response by MDA-MB-231 or MDA-MB-435 cells in the presence of 0.5 μM LPA. However, the addition of PLB did not effect the migration of cells in the presence of 0.5 μM NH-LPA. The non-hydrolysable LPA analog caused an approximately equivalent migratory response as LPA in both cell lines (FIG 3.3). Interestingly, PLB alone decreased the basal migration of both cell lines by about 50%, suggesting that MDA-MB-231 and MDA-MB-435 cells may produce their own LPA and that this might be responsible for the strong basal migration observed in each cell line.

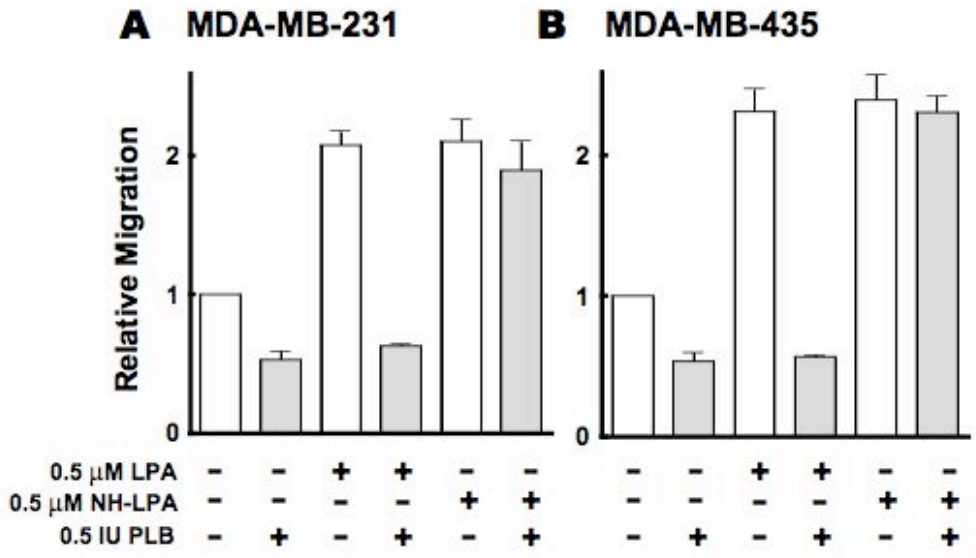

FIGURE 3.3: Migration of MDA-MB-231 and MDA-MB-435 cells in response to LPA is significantly reduced in the presence of phospholipase B. The relative number of MDA-MB-231 cells, Panel A, and MDA-MB-435 cells, Panel B, that migrated per field is shown when the cells were incubated for 3 h with LPA, or the non-hydrolysable analogue of LPA (NH-LPA) in the bottom chamber. Results are expressed relative to the number of cells migrating with basal media alone (RPMI 1640 with 0.1% BSA and 0.2% FBS-C), which is given a value of 1. The results are means ± ranges from 2 independent experiments.

3.3 Autotaxin is Produced by MDA-MB-435 Breast Cancer Cells but Not by MDA-MB-231 or MCF-7 Cells

There are two possible explanations for why MDA-MB-435 cells display an increased migratory response to increasing concentrations of LPC and MDA-MB-231 cells do not. First, there may be a receptor that initiates a migratory stimulus upon LPC binding that MDA-MB-231 cells do not express and instead MDA-MB-435 cells possess this receptor, thus they are sensitive to LPC. Second, MDA-MB-435 could express ATX which would result in the production of LPA from LPC, and the LPA that is produced is able to stimulates cell migration, whereas MDA-MB-231 cells do not express ATX. To find out which mechanism is occurring we measured the ATX expression in our cell lines. We first looked at ATX mRNA expression in MDA-MB-435, MDA-MB-231, and MCF-7 cells. Our MDA-MB-435 cells expressed significantly more ATX mRNA than MDA-MB-231 and MFC-7 cells as shown by real-time RT-PCR analysis (FIG 3.4). We also examined ATX protein expression and activity in the conditioned media and lysates collected from our cell lines. Western Blot analysis of medium from MDA-MB-435 showed marked expression of ATX, whereas ATX was barely detectable in equivalent amounts of medium from MDA-MB-231 and MCF-7 cells (FIG 3.5A,B). Furthermore, in our ATX activity assay we found that, concentrated medium from MDA-MB-231 and MCF-7 cells showed very low ATX activity compared to MDA-MB-435 medium (FIG 3.5C). Western Blot analysis on the cell lysates showed no detectable ATX protein expression for any of our cell lines and there was also no detectable ATX activity

found by fluorescence assay (FIG 3.6), which would imply that ATX is mainly a secreted protein as previously shown [121].

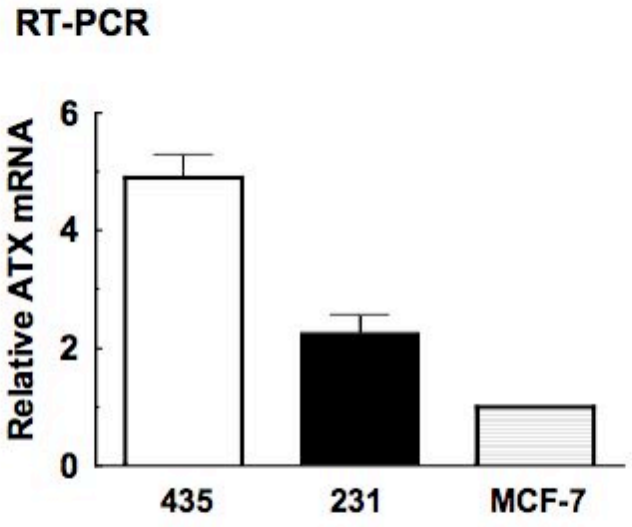

FIGURE 3.4: Expression of ATX mRNA in MDA-MB-435, MDA-MB-231, and MCF-7 cell lines. This is a figure prepared from the work of Nasser Samadi in our lab. The relative mRNA levels of ATX are shown compared to the level of mRNA in MCF-7 cells, which is given a value of 1. Results were normalized to mRNA levels of glyceraldehyde 3-phosphate dehydrogenase (GAPDH) and are means ± SEM from at least 3 independent experiments.

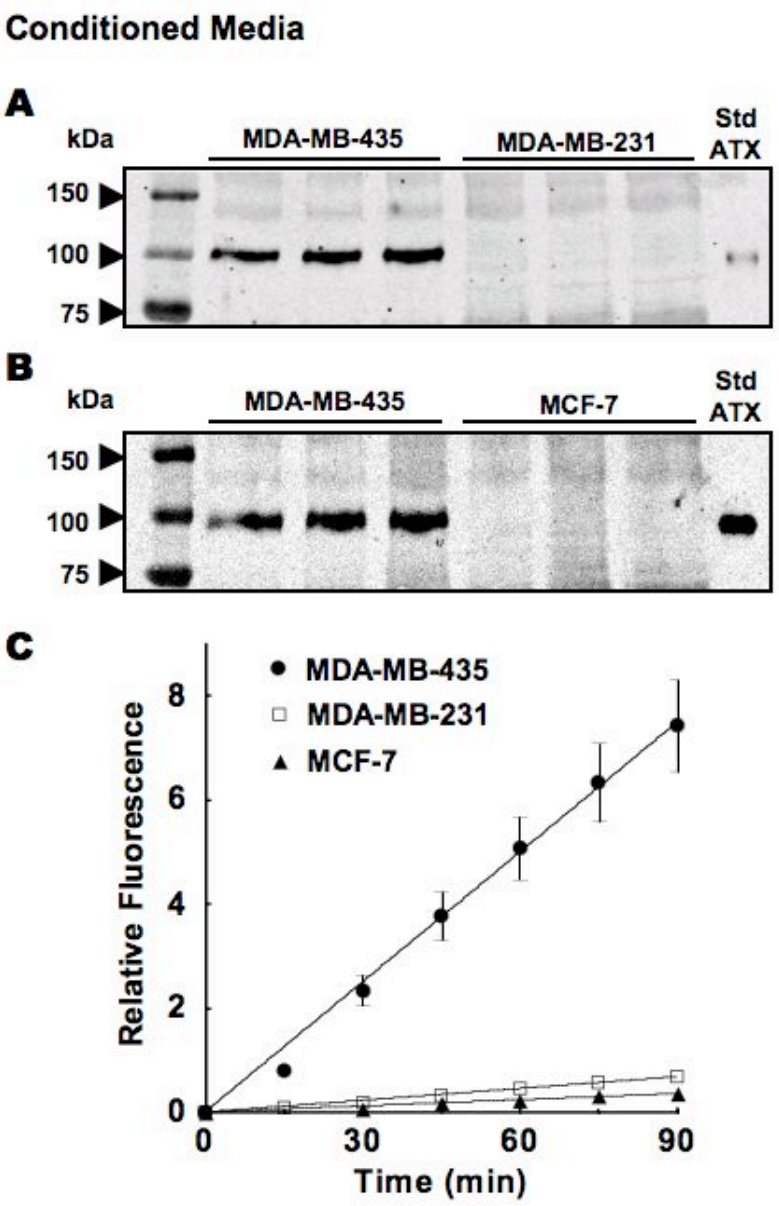

FIGURE 3.5: MDA-MB-435 cells secrete significant amounts of active ATX into the extracellular medium compared to MDA-MB-231, and MCF-7 cells. Panel A shows Western Blot analysis for ATX of concentrated media collected from 3 separate dishes of MDA-MB-435 or MDA-MB-231 cells. Panel B shows a similar experiment where MDA-MB-435 concentrated media is compared against MCF-7 concentrated media. Recombinant ATX was used as a control for both blots. Panel C shows the results from the fluorescence assay for ATX activity of concentrated media collected from MDA-MB-435 (○), MDA-MB-231 (■), or MCF-7 (▲) cells Results are means ± SEM from at least 3 independent experiments.

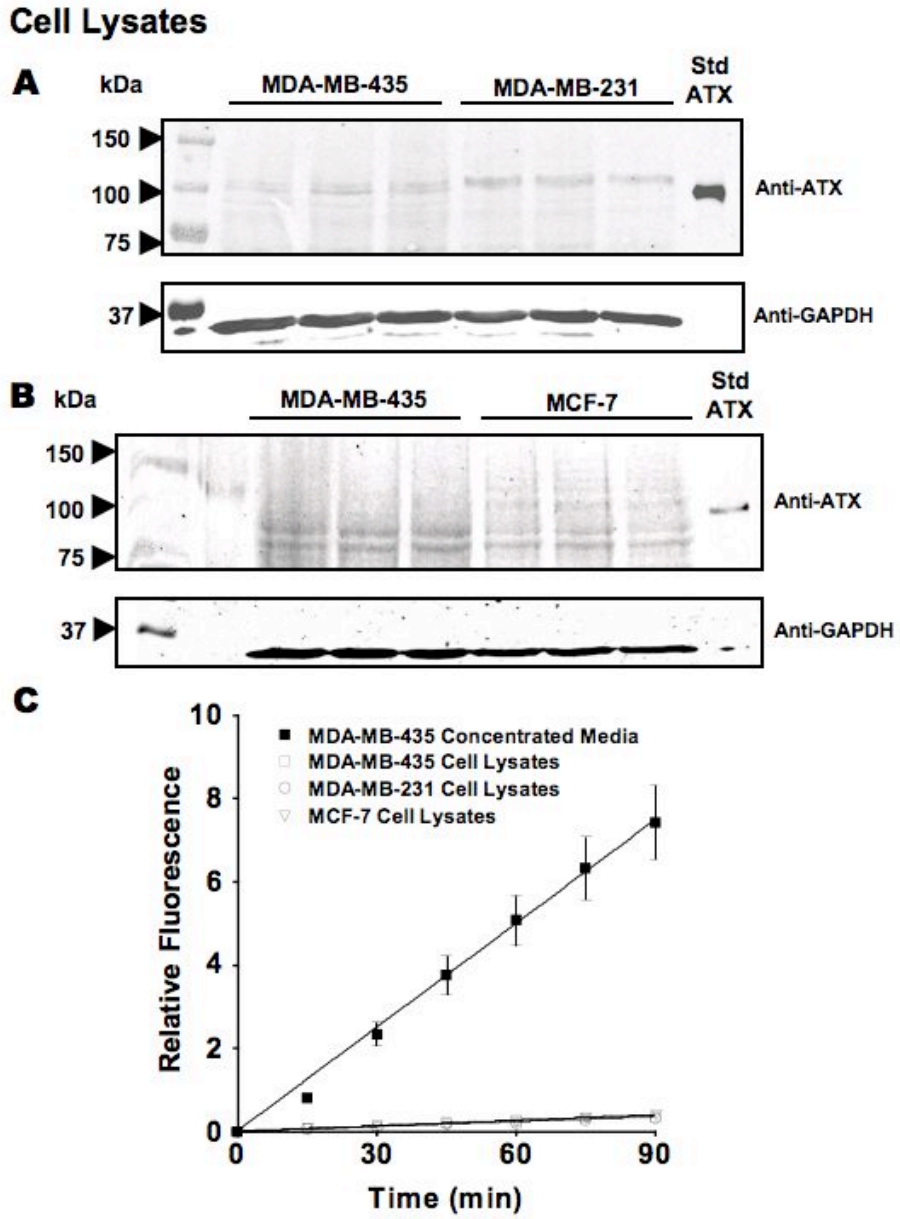

FIGURE 3.6: Autotaxin is not detected in cell lysates from MDA-MB-435, MDA-MB-231, and MCF-7 cell lines. Panel A shows Western Blot analysis of cell lysates for ATX from 3 separate dishes of MDA-MB-435 or MDA-MB-231 cells. Similar experiment in Panel B showing Western Blot analysis of cell lysates from 3 separate dishes of MDA-MB-435 cells again along with MCF-7 cell lysates. Recombinant ATX was used as a standard and housekeeping gene GAPDH was used as a loading control in both experiments. Panel C shows the results from the fluorescence assay for ATX activity on cell lysates of MDA-MB-435 (□), MDA-MB-231 (○), or MCF-7 (▽) cells. Concentrated media from MDA-MB-435 cells (■) was used as a positive control. Results are means ± SEM from at least 3 independent experiments.

3.4 Migration of MDA-MB-435 Cells in the Presence of LPA is Abolished with the Addition of Autotaxin Activity Inhibitors

We measured the migration of MDA-MB-435 cells over a 3 h incubation in the presence or absence of two inhibitors of ATX activity: VPC8a202 and S32826 ([4-(tetradecanoylamino)benzyl] phosphonic acid). At a concentration of 1 μM neither of the inhibitors significantly effected the migration of the MDA-MB-435 cells in basal media alone, likewise the stimulation of migration observed in the presence of 0.5 μM LPA was not effected by the addition of the ATX inhibitors. Although, the stimulation of migration observed in the presence 10 μM LPC was completely abolished with the addition of the inhibitors (FIG 3.7). This would suggest that catalytic activity of ATX is required for the migration of MDA-MB-435 cells towards LPC. To support this conclusion we tested the ATX inhibitors under the conditions of the FS-3 fluorescence assay. We found that VPC8a202 and S32826 inhibited ATX activity in the concentrated media of MDA-MB-435 cells by about 93% and 90% respectively and that VPC8a202 was able to reduce the ATX activity of 65 ng of recombinant ATX by about 95% (FIG 3.8). Detailed kinetic studies on the inhibition of ATX by VPC8a202 using LPC, the natural substrate for ATX, were performed by Jose Tomsig (University of Virginia). It was determined that VPC8a202 acts as a competitive inhibitor of ATX, as expected from a substrate analogue, with a K_i of about 390 nM [122]. This supports that concentrations in the μM range used in our migration experiments are effective in inhibiting ATX and thus the migratory effects of LPC are due to the conversion of LPC to LPA by ATX.

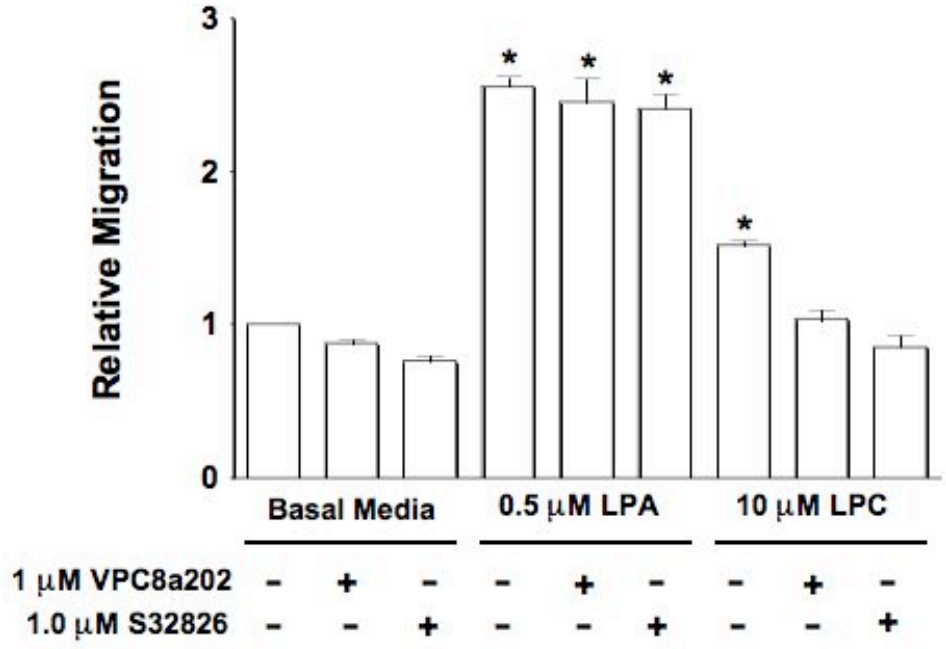

FIGURE 3.7: Inhibition of ATX activity impairs ability of MDA-MB-435 cells to migrate in the presence of LPC. A 4 h incubation was used to measure the migration of MDA-MB-435 cells in the presence of basal media, 0.5 μM LPA, or 10 μM LPC with or without the addition of ATX inhibitors. Both ATX inhibitors, VPC8a202 and S32826, were used at a concentration of 1 μM. The results are expressed relative to the number of cells migrating with only basal media (RPMI 1640 with 0.1% BSA and 0.2% FBS-C), which is given a value of 1. Results are means ± SEM from 3 independent experiments. Statistically significant differences are indicated by: * ($p < 0.01$).

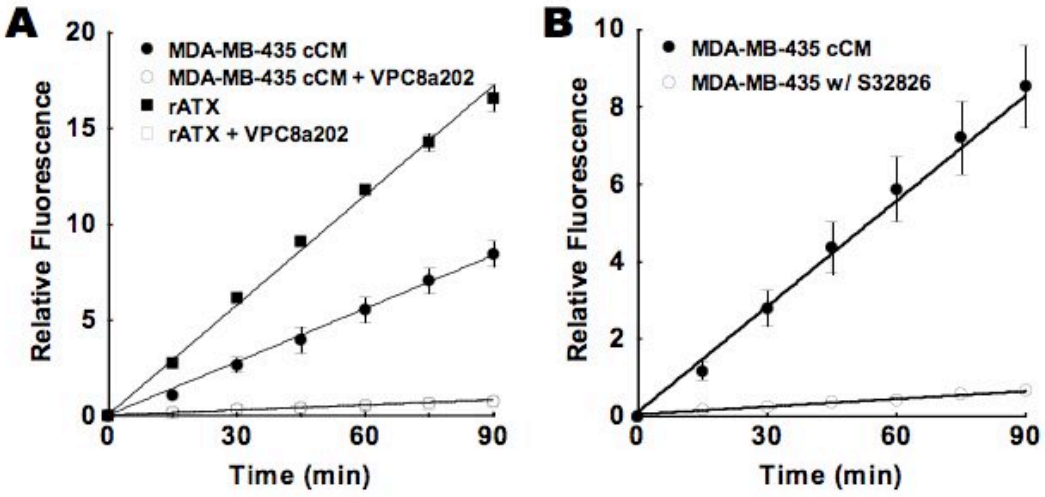

FIGURE 3.8: Inhibition of ATX activity by VPC8a202 and S32826. Panel A shows the results from the fluorescence assay of ATX activity using 65 ng recombinant ATX in the absence (■) or presence of 1 μM VPC8a202 (ATX inhibitor) (□). ATX activity in the concentrated medium (cM) from MDA-MB-435 is also shown in the absence (●) or presence of 1 μM VPC8a202 (○). A separate but similar experiment is shown in Panel B. ATX activity in the concentrated medium from MDA-MB-435 cells is shown in the absence (●) or presence of 1 μM S32836 (○). Error bars indicate the SEM of 3 experimental values.

3.5 Concentrated Medium from MDA-MB-435 Cells Stimulates Cell Migration in the Presence of LPC because of its Autotaxin Activity

To determine why MDA-MB-435 and MDA-MB-231 cells respond differently to LPC we measured the effects of adding media collected from these cells to the bottom well of the migration chamber. Initially we measured the migration of MDA-MB-435 cells over a 3 h incubation using non-concentrated media. The media from either cell line caused an increased migratory response in comparison to that obtained with basal media alone (approximately 75 cells per field). The addition of 10 μM LPC to medium from MDA-MB-435 cells caused an increase in migration, conversely addition of 1 μM ATX inhibitor (VPC8a202) caused a substantial decrease in migration and abolished any. The addition of LPC or VPC8a202 to MDA-MB-231 medium did not significantly alter the number of migrating cells (FIG 3.9). More dramatic results were obtained when collected media was first concentrated approximately 30 x and then was diluted back into RPMI 1640 for migration. MDA-MB-231 cells did not show any significant migration in the presence of LPC and their own concentrated medium. By contrast, a migratory response similar to that obtained with 5% FBS, or 0.5 μM LPA was obtained when concentrated medium from MDA-MB-435 was added to the bottom chamber. This stimulation of migration was completely abolished by the addition of VPC8a202 to the wells (FIG 3.10).

A similar experiment was performed with MDA-MB-435 cells. Addition of concentrated medium from MDA-MB-231 cells had no significant effect on the migration of MDA-MB-435 cell in the presence, or absence of LPC (FIG 3.11).

By contrast, there was a significant stimulation of migration when concentrated medium from the MDA-MB-435 cells themselves was added to the bottom chamber with LPC. Again this response was abolished with the addition of VPC8a202. As a control, we showed that the addition of VPC8a202 did not significantly affect the LPA-induced stimulation of migration for either cell line (FIG 3.10,3.11). This demonstrates that the effect of VPC8a202 was specific for LPC-induced migration.

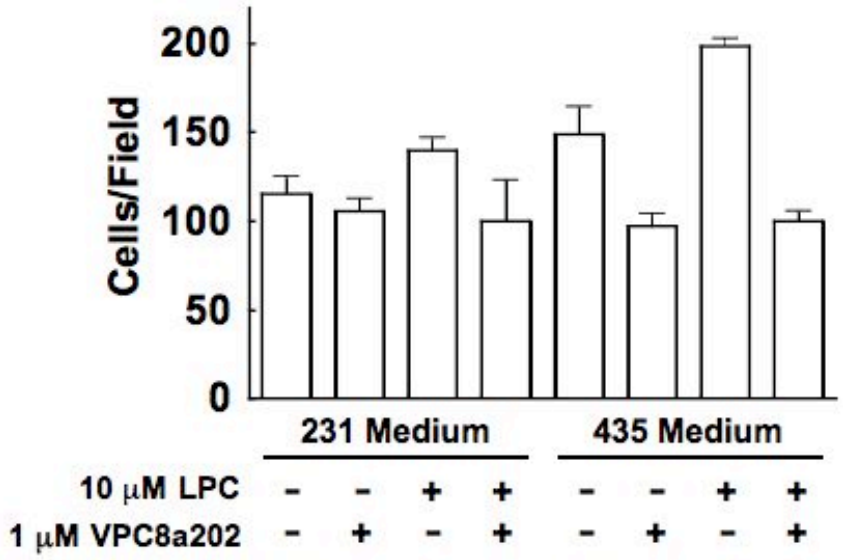

FIGURE 3.9: Migration of MDA-MB-435 cells in the presence of media collected from MDA-MB-435, and MDA-MB-231 cells. Shown is the migration of MDA-MB-435 cells over a 3 h incubation in the presence of media collected from either MDA-MB-435, or MDA-MB-231 cells. This migration was performed in the presence or absence of 10 μM LPC, 1 μM ATX inhibitor (VPC8a202), or both. Results are from one experiment and show means ± S.D. of cells per field from 6 fields.

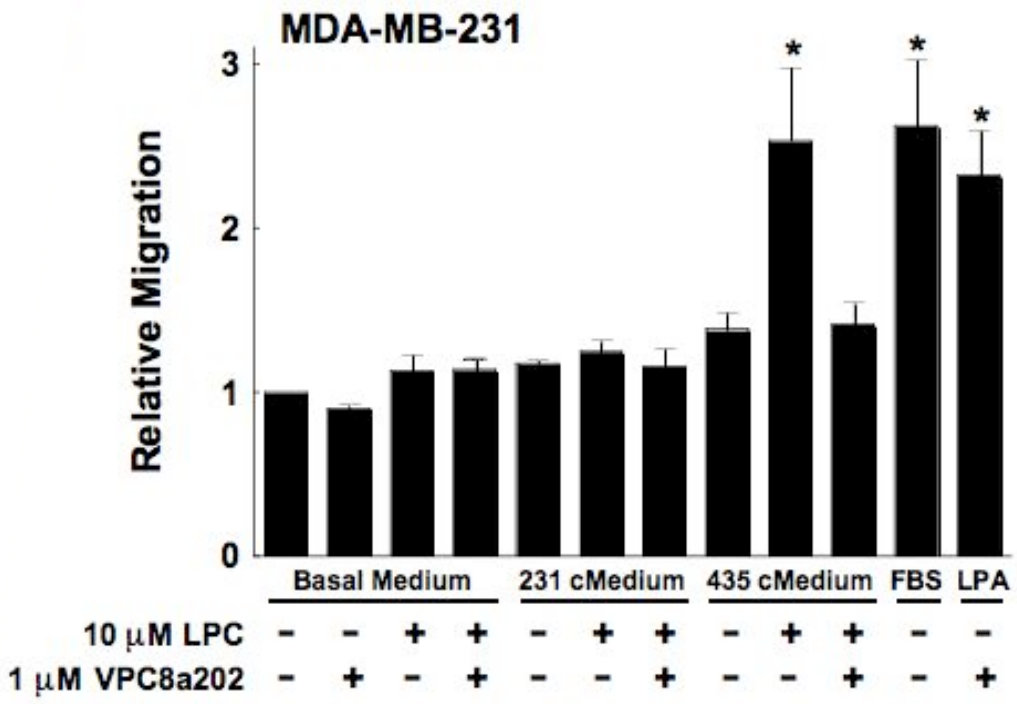

FIGURE 3.10: MDA-MB-231 cells are stimulated to migrate in the presence of LPC and concentrated medium from MDA-MB-435 cells, but not from MDA-MB-231 cells. The migration of MDA-MB-231 cells is shown over 3 h incubation in the presence of basal medium or concentrated medium prepared from either MDA-MB-231 cells (231 cMedium), or from MDA-MB-435 cells (435 cMedium). These experiments were performed in the presence or absence of 10 μM LPC, and/or 1 μM ATX inhibitor (VPC8a202). Migration in the presence of 5% FBS and 0.5 μM LPA plus 1 μM VPC8a202 were used as controls. Migration of MDA-MB-231 cells with only basal media (RPMI 1640 with 0.1% BSA and 0.2% FBS) present was given a value of 1. Results are means ± SEM from at least 3 independent experiments. Statistically significant differences are indicated by: * ($p < 0.01$).

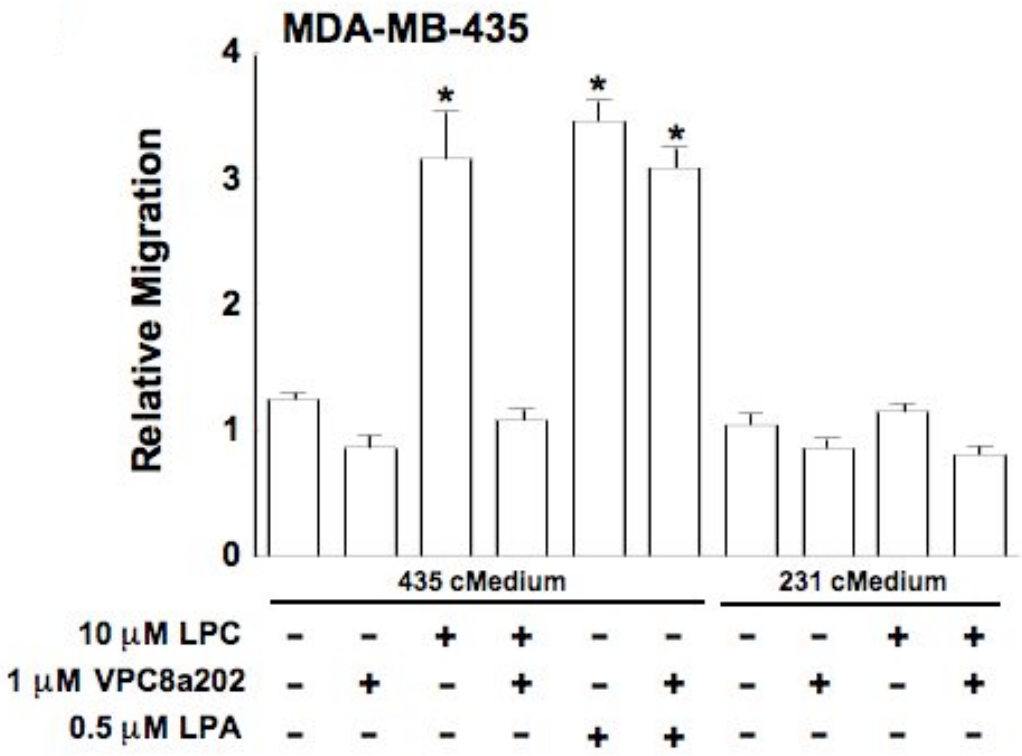

FIGURE 3.11: MDA-MB-435 cells show increased migration in the presence of LPC and concentrated medium collected from MDA-MB-435 cells. The migration of MDA-MB-435 cells is shown over a 3 h incubation in the presence of concentrated medium prepared from either MDA-MB-435 cells (435 cMedium), or from MDA-MB-231 cells (231 cMedium) and in the presence or absence of 10 μM LPC, and/or 1 μM ATX inhibitor (VPC8a202). As a control 0.5 μM LPA and 0.5 μM LPA plus 1 μM VPC8a202 were added to MDA-MB-435 concentrated medium. Migration of MDA-MB-435 cells with only basal media (RPMI 1640 with 0.1% BSA and 0.2% FBS) present was given a value of 1. Results are means ± SEM from at least 3 independent experiments. Statistically significant differences are indicated by: * ($p < 0.01$).

3.6 Expression or Secretion of Autotaxin by MDA-MB-435 Cells is not Effected by Treatment with Autotaxin Inhibitor VPC8a202

Other than inhibiting the catalytic activity of ATX we hypothesized that VPC8a202 may effect the production of ATX as well. To investigate this hypothesis we collected medium from MDA-MB-435 cells, as a control 1 dish of cells received no treatments and 3 separate dishes were treated with 1 μM VPC8a202. Western Blot analysis showed that there were no differences in ATX protein level between media from the control cells or the VPC8a202 treated cells (FIG 3.12). This allowed us to conclude that the presence of VPC8a202 does not effect the production of ATX but simply inhibits its catalytic activity.

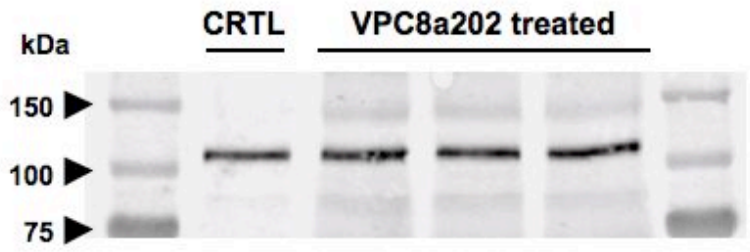

FIGURE 3.12: Treatment of MDA-MB-435 cells with VPC8a202 does not effect production or secretion of ATX into the extracellular medium. MDA-MB-435 cells were treated with starvation media (RPMI 1640 with 0.1% BSA) and 1 μM VPC8a202 for 24 h, dishes were washed and plain media (RPMI 1640) with 1 μM VPC8a202 was added, after another 24 h incubation the media was collected. The same procedure was used in the absence of VPC8a202 to collect media as a control. A Western Blot analysis for ATX is shown of concentrated media collected from 3 separate dishes of VPC8a202 treated MDA-MB-435 cells and 1 dish of untreated cells.

3.7 Knockdown of Autotaxin Expression in MDA-MB-435 Cells Prevents Stimulation of Migration by LPC

To validate results observed with the use of ATX inhibitors, we investigated the requirement for ATX in migration using siRNA to knockdown ATX expression. Treating MDA-MB-435 cells with siRNA for ATX decreased ATX activity by 85% in media collected from siATX treated cells compared to the siControl (siCTRL) treated cells (FIG 3.13A). Furthermore, expression of the ATX protein in conditioned media from siATX treated cells was markedly reduced to levels that were nearly undetectable by Western blot (FIG 3.13B). Thus our experimental procedure was efficient in reducing ATX production by MDA-MB-435 cells.

Over a 3 h incubation no differences were observed in the migration of MDA-MB-435 cells when stimulated with equal amounts of concentrated media collected from siATX, or siCTRL-treated cells. The addition of 10 μM LPC to concentrated media from siCTRL-treated cells caused a substantial increase in the number of migrating cells. By contrast, addition of 10 μM LPC to concentrated medium from siATX-treated cells did not elicit an increased migratory response (FIG 3.14).

In addition, we tested the stimulation of migration with LPC, or LPA on the siRNA-treated cells directly, but using a 6 h incubation for the migration assay. Both the siCTRL and the siATX treated cells migrated to the same extent in the absence of agonist. With the addition of 10 μM LPC a strong stimulation in the migration of siCTRL-treated cells was observed. However, cells treated with

siATX did not respond to LPC stimulation. As a control, we showed that both the siATX and siCTRL-treated cells still showed strong migration in the presence of 0.5 μM LPA. These results emphasize that siATX-treated cells are not migration deficient, but simply no longer respond to LPC (FIG 3.15).

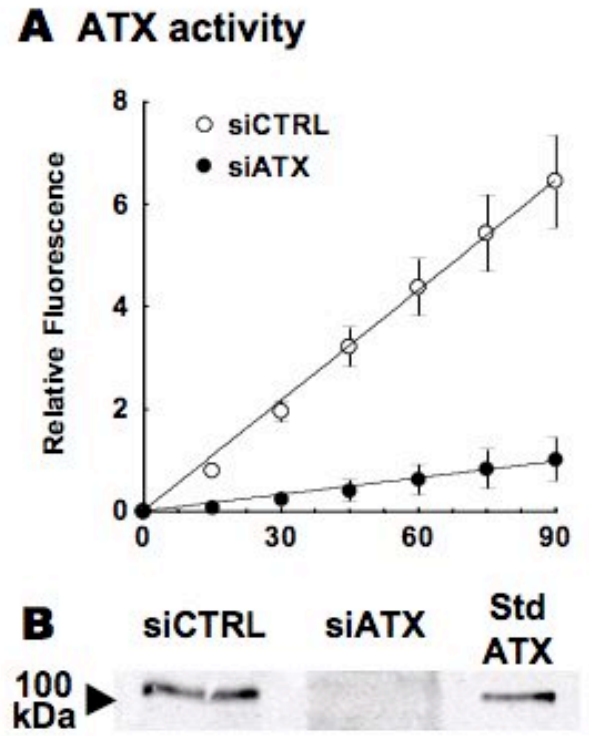

FIGURE 3.13: Knockdown of ATX in MDA-MB-435 cells with siRNA. Concentrated medium was collected from 3 dishes of MDA-MB-435 cells treated with siRNA for ATX (siATX) and 3 dishes treated with control siRNA (siCTRL). Panel A shows a fluorescence assay representing ATX activity in siCTRL concentrated medium (○) and in siATX concentrated medium (●). Error bars indicate the SEM of 3 experimental values. Panel B, Western Blot analysis of a representative sample of concentrated media from siATX and siCTRL treated cells that were probed for ATX. Recombinant ATX was used as a standard.

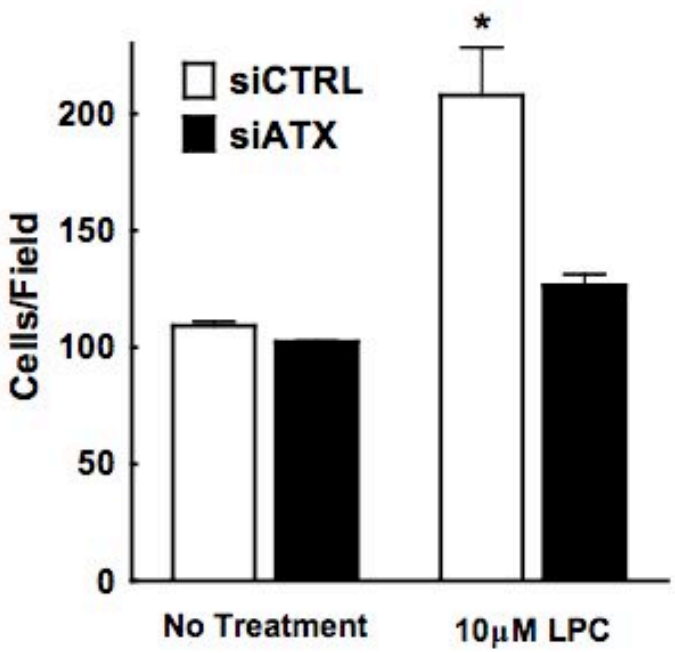

FIGURE 3.14: Knockdown of ATX with siRNA significantly decreases the migratory potential of concentrated medium from MDA-MB-435 cells. The migration of MDA-MB-435 cells is shown over a 3 h incubation in the presence of concentrated medium from siCTRL (white bars) or siATX (dark bars) treated cells in the presence or absence of 10 μM LPC. Results are means ± SEM from 3 independent experiments. Statistically significant differences are indicated by * ($p < 0.01$).

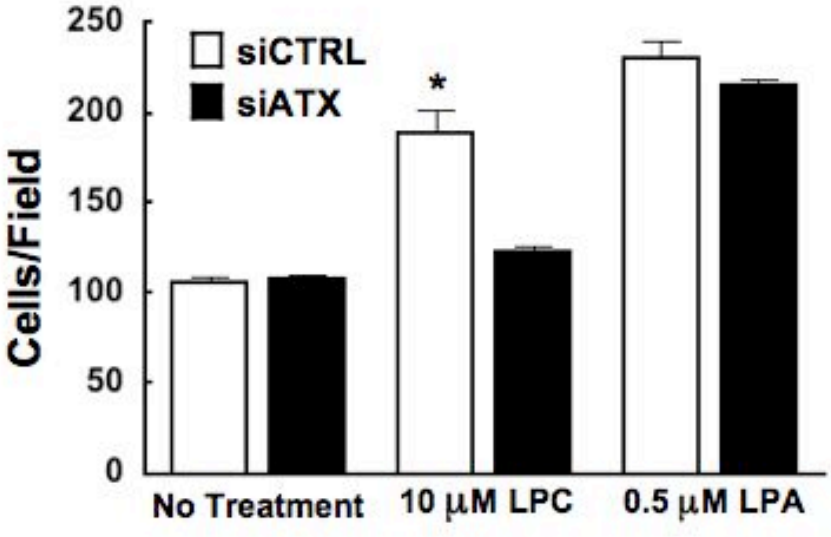

FIGURE 3.15: Knockdown of ATX in MDA-MB-435 cells with siRNA abolishes stimulation of migration by LPC. A 6 h incubation was used to compare the migration of MDA-MB-435 cells that were treated with either siATX or siCTRL. Migration in basal media (RPMI 1640 with 0.1% BSA and 0.2% FBS-C) was compared to migration in the presence of 10 μM LPC or 0.5 μM LPA. Results are means ± ranges from 2 independent experiments.

3.8 LPC Induced Migration of MDA-MB-435 Cells is Inhibited by VPC32183 $LPA_{1/3}$ Receptor Antagonists

These combined results establish that the LPC effect in stimulation cell migration is dependent on the presence of catalytic activity from ATX and LPA production, which could then stimulate migration through LPA receptors. This was supported with the use of VPC32183 in our migration assay, a $LPA_{1/3}$ receptor antagonist [123]. A significant decrease in migration of MDA-MB-435 cells was observed when we added 1 μM VPC32183 to the conditioned media alone (FIG 3.16). Secondly, the migration obtained with LPC in the presence of concentrated medium from MDA-MB-435 cells was abolished by VPC32183. Likewise, the migratory stimulus provided by LPA was greatly reduced by the addition of VPC32183.

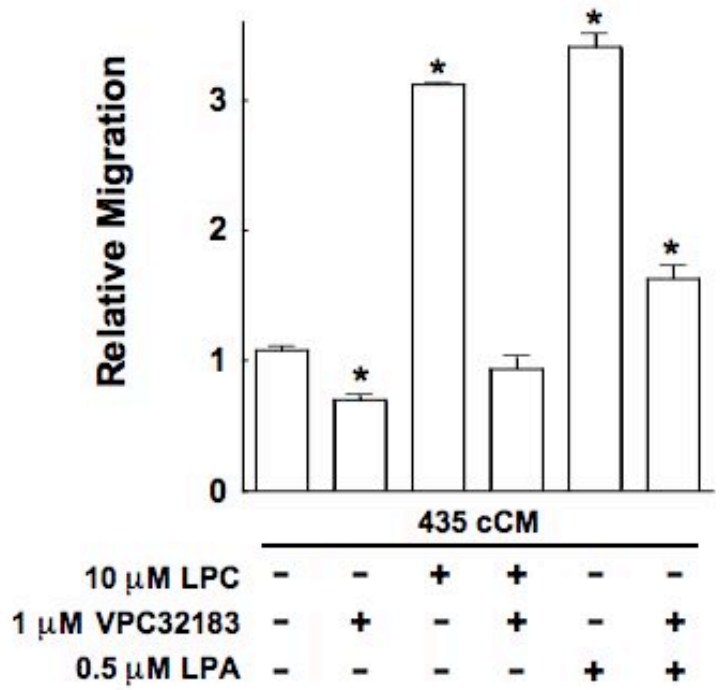

FIGURE 3.16: $LPA_{1/3}$ Receptor antagonist VPC32183 inhibits migration of MDA-MB-435 cells. A 3 h incubation was used to measure the migration of MDA-MB-435 cells in the presence of their own concentrated medium with either LPC or LPA in the presence or absence of the $LPA_{1/3}$ receptor antagonist (VPC32183). Migration in the presence of agonists/antagonists was compared to the number of cells migrating in basal media (RPMI 1640 with 0.1% BSA and 0.2% FBS), which is given a value of 1. Results are means ± SEM from at least 3 independent experiments. Statistically significant differences are indicated by: * ($p < 0.01$).

CHAPTER 4

DISCUSSION AND FUTURE DIRECTIONS

4.1 Discussion

The role of autotaxin in tumourigenesis has been studied intensively in recent years; increased expression of autotaxin has been linked to several malignancies such as; glioblastoma, lung, liver, breast, renal, ovarian, and thyroid cancers [15-21]. In our studies, we worked with three commonly studied cell lines, MDA-MB-231 and MCF-7 breast cancer cells and also MDA-MB-435 cells which were previously thought to be breast cancer cells but now have been identified as melanoma cells [118]. Both MDA-MB-435 and MDA-MB-231 cells exhibited a strong migratory response to serum or LPA. MCF-7 cells, on the other hand, did not migrate in response to LPA and only slightly to serum. Because of this they were not used in further migration experiments since they appeared to be migration deficient without modification [124]. However, they were still used, as comparison, for ATX expression and our Group used then for studies on Taxol-induced apoptosis [125].

MDA-MB-435 cells exhibited a strong migratory response towards LPC, however LPC did not stimulate the migration of MDA-MB-231 cells. We hypothesized that this may be due to differences in expression of the pro-migratory protein, ATX, and therefore, LPC itself, does not induce migration of these cells, but rather its effects are dependent upon metabolism to LPA. Thus we also hypothesized that the inhibition of ATX activity or knockdown of ATX expression should minimize LPC responses.

We were able to show that MDA-MB-435 cells secrete an abundance of ATX into the extracellular environment, whereas conditioned media collected

from MDA-MB-231 and MCF-7 cells had near undetectable levels of ATX. These differences in ATX expression were also reflected in our ATX activity experiments. Interestingly, the expression of ATX mRNA in MDA-MB-231 cells was only slightly less than half that of MDA-MB-435 cells but the mRNA did not translate into an equivalent amount of secreted protein or activity. This suggests that the mRNA transcripts are degraded before translation into protein and/or the protein is degraded shortly after production and is not secreted. Confirmation of ATX being primarily a secreted protein was provided by our experiments with cell lysates from the three cell lines. None of the cell lysates from any of the cell lines showed significant ATX protein expression by western blot and no ATX activity was detected in the fluorescence assay, in the case of MDA-MB-435 cells, this would suggest that ATX is secreted quickly into the extracellular milieu shortly after production.

We were able to demonstrate the effectiveness of the inhibitors in blocking the catalytic activity of ATX through our results from our activity assays using the fluorogenic ATX substrate FS-3 [119]. Also the work of Jose Tomsig (University of Virginia) confirmed the efficacy of VPC8a202 at the concentrations we used in our experiments and with the natural ATX substrate LPC. Thus, we were assured that we were getting a very strong inhibition of ATX activity in our migration experiments. To assure us that VPC8a202 was not preventing the expression of ATX, we collected media from MDA-MB-435 cells in the presence of VPC8a202 and showed by Western blot that its presence did not effect the production of ATX. Another compound, S32826, was shown to be

an effective inhibitor of ATX by fluorescence assay. However, with S32836 here we did not do the same extensive investigations for effects on ATX production or effective concentrations with LPC as a substrate, this compound was studied extensively as an ATX inhibitor [126].

We verified our hypothesis of the necessity of ATX in LPC-induced migration in several experiments. We initially showed that addition of ATX activity inhibitors, VPC8a202 and S32826, prevented the migration of MDA-MB-435 cells in response to LPC specifically and because LPA induced migration was not effected by the presence of inhibitors. In some preliminary migration experiments, addition of LPC to media from MDA-MB-435 cells caused increased migratory response of MDA-MB-435 cells compared to media from MDA-MB-231 cells. However the differences in stimulation were not pronounced, most likely due to the high basal migration observed with either cells' media, probably a result of several pro-migratory factors contained in the conditioned media. To address this issue, we helped to isolate the effects of ATX in the media by first concentrating the condition media approximately 30-fold and then diluting it in plain media before migration. The addition of concentrated medium collected from MDA-MB-435 cells caused significant migration of MDA-MB-231 cells in the presence of LPC. However, no stimulation of migration was observed when MDA-MB-231 media was used instead. Again migration of MDA-MB-435 cells was strongly stimulated in the presence of its own concentrated media and LPC but MDA-MB-231 concentrated media and LPC showed insignificant stimulation of migration. This evidence supports the

hypothesis that ATX is required for LPC induced migration, since MDA-MB-231 media that is ATX deficient was unable to stimulate migration in the presence of LPC. Furthermore, in both of these experiments the stimulation of migration with MDA-MB-435 media and LPC was abolished by the addition of VPC8a202.

In order to support our findings with ATX inhibitors, we used siRNA to knockout expression of ATX in MDA-MB-435 cells. Efficient knockout of ATX expression was confirmed by Western blot and ATX assay on media obtained from siATX treated cells. MDA-MB-435 cells treated with siATX no longer migrated in the presence of LPC, but still migrated at similar levels to siCTRL treated cells in the presence of LPA. Also, addition of LPC to media collected from the siATX treated cells did not significantly stimulate migration above baseline levels.

We then used a $LPA_{1/3}$ receptor antagonist, VPC32183, to further confirm that conversion of LPC to LPA is required to stimulate migration. Addition of VPC32183 to MDA-MB-435 conditioned media blocked migration in response to both LPC- and LPA-induced migration. These results strongly support that the mechanism by which ATX is able to stimulate migration is indirectly through the conversion of LPC to LPA and not directly thought the non-catalytic modification of cell adhesion though its C-terminal region.

Our preliminary experiments with PLB have shown that LPA may be involved in the high basal migration levels of both MDA-MB-435 and MDA-MB-231 cells. The presence of PLB decreased the migration of both cell lines to approximately half of that with basal medium alone. This result suggests that

both MDA-MB-435 and MDA-MB-231 have some endogenous production of LPA. In MDA-MB-435 cells LPA production of maybe secondary to LPC production and ATX activity. An investigation into the production or secretion of LPC and LPA by MDA-MB-435 cells would prove helpful in understanding this result. It would also be interesting to investigate LPA production by MDA-MB-231 cells, the mechanism could not occur through LPC because we have shown that these cells do not produce significant ATX and they do not migrate in response to LPC stimulation. The possibility of endogenous LPA production in MDA-MB-435 cells is further validated in our migration experiments with $LPA_{1/3}$ receptor antagonist VPC32183. The addition of the agonist, even in the presence of concentrated media from MDA-MB-435 cells, caused a significant decrease in migration compare to migration with basal media.

Other studies have proposed that LPC can directly stimulate migration through action on G2A and GPR4 receptors [57-61, 127] but much of work is now in question [63]. It is proposed now that G2A and GPR4 are proton-sensing receptors and that instead are negatively regulated by LPC [62, 63]. Our work has not found any evidence of a stimulatory effect on migration by LPC alone; a migratory stimulus was only achieved with conversion to LPA through the actions of ATX. These findings are in accordance with an independent publication that showed inhibition of ATX activity was able to block cell migration and invasion in melanoma cells [101]. Likewise, we were able to show that the action of ATX is required to allow LPC to protect MCF-7 and MDA-MB-435 cells from Taxol-induced apoptosis [125].

In summary, this thesis shows that the conversion of LPC to LPA by the enzymatic activity of ATX is necessary to achieve LPC induced migration in two common cancer cell lines. We established this as follows: (a) First, MDA-MB-435 cells with strong expression of ATX showed significant migration in the presence of LPC that the did not occur with MDA-MB-231 cells; (b) Second, we were able to prevent LPC induced migration by using siRNA to suppress the expression of ATX in MDA-MB-435 cells; (c) Third, any induction of migration in the presence of LPC was blocked by the addition of two different ATX inhibitors; (d) Lastly, the use of an $LPA_{1/3}$ receptor antagonist prevent migration in the presence of LPC.

As mentioned previously we now know that extracellular LPA promotes tumour growth and metastasis and that several aggressive cancers express high levels of ATX. My work shows that restricting the activity of ATX and signaling by LPA should provide potentially valuable targets for further cancer research. We propose that because of the relatively high concentrations of LPC in extracellular fluids, the ability to prevent the formation of LPA by ATX could prove to be a strong adjuvant to treating cancers by surgery and chemotherapy therapy.

4.2 Future Directions

Several papers have been published regarding autotaxin in the last few years since the majority of this work was completed. However there are still several questions that can be expanded upon from findings in this thesis. Knowing that MDA-MB-231 cells do not express ATX but do have significant levels of ATX mRNA it would be useful to investigate the regulation of the ATX mRNA transcripts in these cells. Currently very little is known about the regulation of ATX expression. It is also possible that MDA-MB-231 cells mainly express the enzymaticaly inactive α isoform of ATX. Which may explain the lack of ATX activity but presence of ATX mRNA in MDA-MB-231 cells. This could be determined by the isolation and sequencing of the mRNA transcripts using reverse transcriptase and random primers.

Our preliminary work with PLB and the $LPA_{1/3}$ receptor antagonist suggests that the basal migration of MDA-MB-231 is in part due to LPA induced migration. This work demonstrates that ATX is not the source of LPA in MDA-MB-231 cells therefore suggesting there is an alternate process for the endogenous production of LPA in these cells. Production may occur through the PLA_2 or another undisclosed pathway and would be of worth to investigate further. This could be uncovered through the tagging and tracking of metabolites with radioactive molecules.

As it stands, however, an essential step required to advance this area of research would be to ultimately find viable ATX inhibitors that could be used in animal models. Then the effects of blocking ATX in regards to tumour growth

and metastasis could be studied in vivo. In order for the inhibitors to be used in this capacity they would need to be bioavailable and non-toxic at levels used for tumour suppression. With the recent development of transgenic mice that overexpress either ATX or one of the three main LPA receptors we now have excellent models to test new ATX inhibitors [116]. These mice were shown to have increased invasive and metastatic mammary carcinomas, thus the reversal or prevention of invasiveness and metastasis with administration of ATX inhibitors would provide strong evidence for a therapeutic advantage of these inhibitors in cancer treatment.

REFERENCES

1. Fidler, I.J., *The organ microenvironment and cancer metastasis.* Differentiation, 2002. **70**(9-10): p. 498-505.
2. Fidler, I.J., *Critical determinants of metastasis.* Semin Cancer Biol, 2002. **12**(2): p. 89-96.
3. Fidler, I.J., *The pathogenesis of cancer metastasis: the 'seed and soil' hypothesis revisited.* Nat Rev Cancer, 2003. **3**(6): p. 453-8.
4. Chiang, A.C. and J. Massague, *Molecular basis of metastasis.* N Engl J Med, 2008. **359**(26): p. 2814-23.
5. Ariztia, E.V., et al., *The tumor microenvironment: key to early detection.* Crit Rev Clin Lab Sci, 2006. **43**(5-6): p. 393-425.
6. Witz, I.P., *The tumour microenvironment--introduction.* Semin Cancer Biol, 2002. **12**(2): p. 87-8.
7. Stracke, M.L., et al., *Identification, purification, and partial sequence analysis of autotaxin, a novel motility-stimulating protein.* J Biol Chem, 1992. **267**(4): p. 2524-9.
8. Murata, J., et al., *cDNA cloning of the human tumor motility-stimulating protein, autotaxin, reveals a homology with phosphodiesterases.* J Biol Chem, 1994. **269**(48): p. 30479-84.
9. Moolenaar, W.H., *Lysophospholipids in the limelight: autotaxin takes center stage.* J Cell Biol, 2002. **158**(2): p. 197-9.
10. Clair, T., et al., *Autotaxin is an exoenzyme possessing 5'-nucleotide phosphodiesterase/ATP pyrophosphatase and ATPase activities.* J Biol Chem, 1997. **272**(2): p. 996-1001.
11. Tokumura, A., et al., *Production of lysophosphatidic acid by lysophospholipase D in incubated plasma of spontaneously hypertensive rats and Wistar Kyoto rats.* Life Sci, 1999. **65**(3): p. 245-53.
12. Umezu-Goto, M., et al., *Autotaxin has lysophospholipase D activity leading to tumor cell growth and motility by lysophosphatidic acid production.* J Cell Biol, 2002. **158**(2): p. 227-33.
13. Jansen, S., et al., *Proteolytic maturation and activation of autotaxin (NPP2), a secreted metastasis-enhancing lysophospholipase D.* J Cell Sci, 2005. **118**(Pt 14): p. 3081-9.
14. Yuelling, L.M. and B. Fuss, *Autotaxin (ATX): a multi-functional and multi-modular protein possessing enzymatic lysoPLD activity and matricellular properties.* Biochim Biophys Acta, 2008. **1781**(9): p. 525-30.
15. Kishi, Y., et al., *Autotaxin is overexpressed in glioblastoma multiforme and contributes to cell motility of glioblastoma by converting lysophosphatidylcholine to lysophosphatidic acid.* J Biol Chem, 2006. **281**(25): p. 17492-500.

16. Yang, Y., et al., *Autotaxin expression in non-small-cell lung cancer.* Am J Respir Cell Mol Biol, 1999. **21**(2): p. 216-22.
17. Zhang, G., et al., *Expression of autotaxin mRNA in human hepatocellular carcinoma.* Chin Med J (Engl), 1999. **112**(4): p. 330-2.
18. Yang, S.Y., et al., *Expression of autotaxin (NPP-2) is closely linked to invasiveness of breast cancer cells.* Clin Exp Metastasis, 2002. **19**(7): p. 603-8.
19. Stassar, M.J., et al., *Identification of human renal cell carcinoma associated genes by suppression subtractive hybridization.* Br J Cancer, 2001. **85**(9): p. 1372-82.
20. Tokumura, A., et al., *Peritoneal fluids from patients with certain gynecologic tumor contain elevated levels of bioactive lysophospholipase D activity.* Life Sci, 2007. **80**(18): p. 1641-9.
21. Kehlen, A., et al., *Expression, regulation and function of autotaxin in thyroid carcinomas.* Int J Cancer, 2004. **109**(6): p. 833-8.
22. Nam, S.W., et al., *Autotaxin (ATX), a potent tumor motogen, augments invasive and metastatic potential of ras-transformed cells.* Oncogene, 2000. **19**(2): p. 241-7.
23. So, J., et al., *LPA-induced epithelial ovarian cancer (EOC) in vitro invasion and migration are mediated by VEGF receptor-2 (VEGF-R2).* Gynecol Oncol, 2005. **97**(3): p. 870-8.
24. Nam, S.W., et al., *Autotaxin (NPP-2), a metastasis-enhancing motogen, is an angiogenic factor.* Cancer Res, 2001. **61**(18): p. 6938-44.
25. Ptaszynska, M.M., et al., *Positive feedback between vascular endothelial growth factor-A and autotaxin in ovarian cancer cells.* Mol Cancer Res, 2008. **6**(3): p. 352-63.
26. van Meeteren, L.A., et al., *Autotaxin, a secreted lysophospholipase D, is essential for blood vessel formation during development.* Mol Cell Biol, 2006. **26**(13): p. 5015-22.
27. Tanaka, M., et al., *Autotaxin stabilizes blood vessels and is required for embryonic vasculature by producing lysophosphatidic acid.* J Biol Chem, 2006. **281**(35): p. 25822-30.
28. van Meeteren, L.A. and W.H. Moolenaar, *Regulation and biological activities of the autotaxin-LPA axis.* Prog Lipid Res, 2007. **46**(2): p. 145-60.
29. Fox, M.A., et al., *Phosphodiesterase-I alpha/autotaxin controls cytoskeletal organization and FAK phosphorylation during myelination.* Mol Cell Neurosci, 2004. **27**(2): p. 140-50.
30. Mazereeuw-Hautier, J., et al., *Production of lysophosphatidic acid in blister fluid: involvement of a lysophospholipase D activity.* J Invest Dermatol, 2005. **125**(3): p. 421-7.
31. Pamuklar, Z., et al., *Autotaxin/lysopholipase D and lysophosphatidic acid regulate murine hemostasis and thrombosis.* J Biol Chem, 2009. **284**(11): p. 7385-94.

32. Georas, S.N., *Lysophosphatidic acid and autotaxin: emerging roles in innate and adaptive immunity.* Immunol Res, 2009.
33. Li, S. and J. Zhang, *Lipopolysaccharide induces autotaxin expression in human monocytic THP-1 cells.* Biochem Biophys Res Commun, 2009. **378**(2): p. 264-8.
34. Zhao, C., et al., *Regulation of lysophosphatidic acid receptor expression and function in human synoviocytes: implications for rheumatoid arthritis?* Mol Pharmacol, 2008. **73**(2): p. 587-600.
35. Ferry, G., et al., *Autotaxin is released from adipocytes, catalyzes lysophosphatidic acid synthesis, and activates preadipocyte proliferation. Up-regulated expression with adipocyte differentiation and obesity.* J Biol Chem, 2003. **278**(20): p. 18162-9.
36. Mori, K., et al., *Submucosal connective tissue-type mast cells contribute to the production of lysophosphatidic acid (LPA) in the gastrointestinal tract through the secretion of autotaxin (ATX)/lysophospholipase D (lysoPLD).* Virchows Arch, 2007. **451**(1): p. 47-56.
37. Inoue, M., et al., *Autotaxin, a synthetic enzyme of lysophosphatidic acid (LPA), mediates the induction of nerve-injured neuropathic pain.* Mol Pain, 2008. **4**: p. 6.
38. Watanabe, N., et al., *Both plasma lysophosphatidic acid and serum autotaxin levels are increased in chronic hepatitis C.* J Clin Gastroenterol, 2007. **41**(6): p. 616-23.
39. Boutin, J.A. and G. Ferry, *Autotaxin.* Cell Mol Life Sci, 2009.
40. Giganti, A., et al., *Murine and human autotaxin alpha, beta, and gamma isoforms: gene organization, tissue distribution, and biochemical characterization.* J Biol Chem, 2008. **283**(12): p. 7776-89.
41. Dennis, J., L. Nogaroli, and B. Fuss, *Phosphodiesterase-Ialpha/autotaxin (PD-Ialpha/ATX): a multifunctional protein involved in central nervous system development and disease.* J Neurosci Res, 2005. **82**(6): p. 737-42.
42. Fox, M.A., et al., *Phosphodiesterase-Ialpha/autotaxin: a counteradhesive protein expressed by oligodendrocytes during onset of myelination.* Mol Cell Neurosci, 2003. **23**(3): p. 507-19.
43. Lee, J., et al., *Enzymatic activation of autotaxin by divalent cations without EF-hand loop region involvement.* Biochem Pharmacol, 2001. **62**(2): p. 219-24.
44. Gijsbers, R., et al., *The hydrolysis of lysophospholipids and nucleotides by autotaxin (NPP2) involves a single catalytic site.* FEBS Lett, 2003. **538**(1-3): p. 60-4.
45. Xie, Y. and K.E. Meier, *Lysophospholipase D and its role in LPA production.* Cell Signal, 2004. **16**(9): p. 975-81.
46. Clair, T., et al., *Autotaxin hydrolyzes sphingosylphosphorylcholine to produce the regulator of migration, sphingosine-1-phosphate.* Cancer Res, 2003. **63**(17): p. 5446-53.

47. Brindley, D.N., *Lipid phosphate phosphatases and related proteins: signaling functions in development, cell division, and cancer.* J Cell Biochem, 2004. **92**(5): p. 900-12.
48. Goetzl, E.J., J.J. Liao, and M.C. Huang, *Regulation of the roles of sphingosine 1-phosphate and its type 1 G protein-coupled receptor in T cell immunity and autoimmunity.* Biochim Biophys Acta, 2008. **1781**(9): p. 503-7.
49. Brindley, D.N., *Hepatic secretion of lysphosphatidylcholine: a novel transport system for polyunsaturated fatty acids and choline.* J. Nutr. Biochem., 1993. **4**: p. 442-449.
50. van Meeteren, L.A., et al., *Inhibition of autotaxin by lysophosphatidic acid and sphingosine 1-phosphate.* J Biol Chem, 2005. **280**(22): p. 21155-61.
51. Neidlinger, N.A., et al., *Hydrolysis of phosphatidylserine-exposing red blood cells by secretory phospholipase A2 generates lysophosphatidic acid and results in vascular dysfunction.* J Biol Chem, 2006. **281**(2): p. 775-81.
52. Fourcade, O., et al., *Secretory phospholipase A2 generates the novel lipid mediator lysophosphatidic acid in membrane microvesicles shed from activated cells.* Cell, 1995. **80**(6): p. 919-27.
53. Moolenaar, W.H., L.A. van Meeteren, and B.N. Giepmans, *The ins and outs of lysophosphatidic acid signaling.* Bioessays, 2004. **26**(8): p. 870-81.
54. Aoki, J., et al., *Serum lysophosphatidic acid is produced through diverse phospholipase pathways.* J Biol Chem, 2002. **277**(50): p. 48737-44.
55. Aoki, J., A. Inoue, and S. Okudaira, *Two pathways for lysophosphatidic acid production.* Biochim Biophys Acta, 2008. **1781**(9): p. 513-8.
56. Matsumoto, T., T. Kobayashi, and K. Kamata, *Role of lysophosphatidylcholine (LPC) in atherosclerosis.* Curr Med Chem, 2007. **14**(30): p. 3209-20.
57. Radu, C.G., et al., *T cell chemotaxis to lysophosphatidylcholine through the G2A receptor.* Proc Natl Acad Sci U S A, 2004. **101**(1): p. 245-50.
58. Zhu, K., et al., *Sphingosylphosphorylcholine and lysophosphatidylcholine are ligands for the G protein-coupled receptor GPR4.* J Biol Chem, 2001. **276**(44): p. 41325-35.
59. Rikitake, Y., et al., *Expression of G2A, a receptor for lysophosphatidylcholine, by macrophages in murine, rabbit, and human atherosclerotic plaques.* Arterioscler Thromb Vasc Biol, 2002. **22**(12): p. 2049-53.
60. Kabarowski, J.H., et al., *Lysophosphatidylcholine as a ligand for the immunoregulatory receptor G2A.* Science, 2001. **293**(5530): p. 702-5.
61. Lin, P. and R.D. Ye, *The lysophospholipid receptor G2A activates a specific combination of G proteins and promotes apoptosis.* J Biol Chem, 2003. **278**(16): p. 14379-86.

62. Murakami, N., et al., *G2A is a proton-sensing G-protein-coupled receptor antagonized by lysophosphatidylcholine.* J Biol Chem, 2004. **279**(41): p. 42484-91.
63. Seuwen, K., M.G. Ludwig, and R.M. Wolf, *Receptors for protons or lipid messengers or both?* J Recept Signal Transduct Res, 2006. **26**(5-6): p. 599-610.
64. Kabarowski, J.H., *G2A and LPC: Regulatory functions in immunity.* Prostaglandins Other Lipid Mediat, 2009.
65. Siess, W. and G. Tigyi, *Thrombogenic and atherogenic activities of lysophosphatidic acid.* J Cell Biochem, 2004. **92**(6): p. 1086-94.
66. Lynch, K.R., *Lysophospholipid receptor nomenclature.* Biochim Biophys Acta, 2002. **1582**(1-3): p. 70-1.
67. Noguchi, K., S. Ishii, and T. Shimizu, *Identification of p2y9/GPR23 as a novel G protein-coupled receptor for lysophosphatidic acid, structurally distant from the Edg family.* J Biol Chem, 2003. **278**(28): p. 25600-6.
68. Lee, C.W., et al., *GPR92 as a New G12/13- and Gq-coupled Lysophosphatidic Acid Receptor That Increases cAMP, LPA5.* J Biol Chem, 2006. **281**(33): p. 23589-97.
69. Pasternack, S.M., et al., *G protein-coupled receptor P2Y5 and its ligand LPA are involved in maintenance of human hair growth.* Nat Genet, 2008. **40**(3): p. 329-34.
70. Tabata, K., et al., *The orphan GPCR GPR87 was deorphanized and shown to be a lysophosphatidic acid receptor.* Biochem Biophys Res Commun, 2007. **363**(3): p. 861-6.
71. Meyer zu Heringdorf, D. and K.H. Jakobs, *Lysophospholipid receptors: signalling, pharmacology and regulation by lysophospholipid metabolism.* Biochim Biophys Acta, 2007. **1768**(4): p. 923-40.
72. Rudge, S.A. and M.J. Wakelam, *Inter-regulatory dynamics of phospholipase D and the actin cytoskeleton.* Biochim Biophys Acta, 2009. **1791**(9): p. 856-61.
73. McDermott, M., M.J. Wakelam, and A.J. Morris, *Phospholipase D.* Biochem Cell Biol, 2004. **82**(1): p. 225-53.
74. Marrache, A.M., et al., *Intracellular signaling of lipid mediators via cognate nuclear G protein-coupled receptors.* Endothelium, 2005. **12**(1-2): p. 63-72.
75. McIntyre, T.M., et al., *Identification of an intracellular receptor for lysophosphatidic acid (LPA): LPA is a transcellular PPARgamma agonist.* Proc Natl Acad Sci U S A, 2003. **100**(1): p. 131-6.
76. Simon, M.F., et al., *Lysophosphatidic acid inhibits adipocyte differentiation via lysophosphatidic acid 1 receptor-dependent down-regulation of peroxisome proliferator-activated receptor gamma2.* J Biol Chem, 2005. **280**(15): p. 14656-62.
77. Gardell, S.E., A.E. Dubin, and J. Chun, *Emerging medicinal roles for lysophospholipid signaling.* Trends Mol Med, 2006. **12**(2): p. 65-75.

78. Chen, M., L.N. Towers, and K.L. O'Connor, *LPA2 (EDG4) mediates Rho-dependent chemotaxis with lower efficacy than LPA1 (EDG2) in breast carcinoma cells.* Am J Physiol Cell Physiol, 2007. **292**(5): p. C1927-33.
79. Pilquil, C., et al., *Lipid phosphate phosphatase-1 regulates lysophosphatidate-induced fibroblast migration by controlling phospholipase D2-dependent phosphatidate generation.* J Biol Chem, 2006. **281**(50): p. 38418-29.
80. Gustin, C., M. Van Steenbrugge, and M. Raes, *LPA modulates monocyte migration directly and via LPA-stimulated endothelial cells.* Am J Physiol Cell Physiol, 2008. **295**(4): p. C905-14.
81. Shida, D., et al., *Lysophosphatidic acid (LPA) enhances the metastatic potential of human colon carcinoma DLD1 cells through LPA1.* Cancer Res, 2003. **63**(7): p. 1706-11.
82. Hama, K., et al., *Lysophosphatidic acid and autotaxin stimulate cell motility of neoplastic and non-neoplastic cells through LPA1.* J Biol Chem, 2004. **279**(17): p. 17634-9.
83. Komachi, M., et al., *LPA1 receptors mediate stimulation, whereas LPA2 receptors mediate inhibition, of migration of pancreatic cancer cells in response to lysophosphatidic acid and malignant ascites.* Carcinogenesis, 2009. **30**(3): p. 457-65.
84. Ren, J., et al., *Lysophosphatidic acid is constitutively produced by human peritoneal mesothelial cells and enhances adhesion, migration, and invasion of ovarian cancer cells.* Cancer Res, 2006. **66**(6): p. 3006-14.
85. Nobes, C.D. and A. Hall, *Rho GTPases control polarity, protrusion, and adhesion during cell movement.* J Cell Biol, 1999. **144**(6): p. 1235-44.
86. Raftopoulou, M. and A. Hall, *Cell migration: Rho GTPases lead the way.* Dev Biol, 2004. **265**(1): p. 23-32.
87. Worthylake, R.A., et al., *RhoA is required for monocyte tail retraction during transendothelial migration.* J Cell Biol, 2001. **154**(1): p. 147-60.
88. Brindley, D.N. and C. Pilquil, *Lipid phosphate phosphatases and signaling.* J Lipid Res, 2009. **50 Suppl**: p. S225-30.
89. Brindley, D.N., et al., *Lipid phosphate phosphatases regulate signal transduction through glycerolipids and sphingolipids.* Biochim Biophys Acta, 2002. **1582**(1-3): p. 33-44.
90. Tanyi, J.L., et al., *The human lipid phosphate phosphatase-3 decreases the growth, survival, and tumorigenesis of ovarian cancer cells: validation of the lysophosphatidic acid signaling cascade as a target for therapy in ovarian cancer.* Cancer Res, 2003. **63**(5): p. 1073-82.
91. Tanyi, J.L., et al., *Role of decreased levels of lipid phosphate phosphatase-1 in accumulation of lysophosphatidic acid in ovarian cancer.* Clin Cancer Res, 2003. **9**(10 Pt 1): p. 3534-45.

92. Smyth, S.S., et al., *Lipid phosphate phosphatases regulate lysophosphatidic acid production and signaling in platelets: studies using chemical inhibitors of lipid phosphate phosphatase activity.* J Biol Chem, 2003. **278**(44): p. 43214-23.
93. Simon, M.F., et al., *Expression of ectolipid phosphate phosphohydrolases in 3T3F442A preadipocytes and adipocytes. Involvement in the control of lysophosphatidic acid production.* J Biol Chem, 2002. **277**(26): p. 23131-6.
94. Yue, J., et al., *Mice with transgenic overexpression of lipid phosphate phosphatase-1 display multiple organotypic deficits without alteration in circulating lysophosphatidate level.* Cell Signal, 2004. **16**(3): p. 385-99.
95. Tomsig, J.L., et al., *Lipid phosphate phosphohydrolase type 1 (LPP1) degrades extracellular lysophosphatidic acid in vivo.* Biochem J, 2009. **419**(3): p. 611-8.
96. Brindley, D.N., et al., *Phosphatidate degradation: Phosphatidate phosphatases (lipins) and lipid phosphate phosphatases.* Biochim Biophys Acta, 2009.
97. Gorshkova, I., et al., *Protein kinase C-epsilon regulates sphingosine 1-phosphate-mediated migration of human lung endothelial cells through activation of phospholipase D2, protein kinase C-zeta, and Rac1.* J Biol Chem, 2008. **283**(17): p. 11794-806.
98. Pyne, S., K.C. Kong, and P.I. Darroch, *Lysophosphatidic acid and sphingosine 1-phosphate biology: the role of lipid phosphate phosphatases.* Semin Cell Dev Biol, 2004. **15**(5): p. 491-501.
99. Jansen, S., et al., *Rapid clearance of the circulating metastatic factor autotaxin by the scavenger receptors of liver sinusoidal endothelial cells.* Cancer Lett, 2009.
100. Baker, D.L., et al., *Carba analogs of cyclic phosphatidic acid are selective inhibitors of autotaxin and cancer cell invasion and metastasis.* J Biol Chem, 2006. **281**(32): p. 22786-93.
101. Saunders, L.P., et al., *Identification of small-molecule inhibitors of autotaxin that inhibit melanoma cell migration and invasion.* Mol Cancer Ther, 2008. **7**(10): p. 3352-62.
102. Samadi, N., et al., *Autotaxin protects MCF-7 breast cancer and MDA-MB-435 melanoma cells against Taxol-induced apoptosis.* Oncogene, 2009. **28**(7): p. 1028-39.
103. Zhang, H., et al., *Dual Activity Lysophosphatidic Acid Receptor Pan-Antagonist/Autotaxin Inhibitor Reduces Breast Cancer Cell Migration In vitro and Causes Tumor Regression In vivo.* Cancer Res, 2009. **69**(13): p. 5441-9.

104. Xu, Y., et al., *Lysophospholipids activate ovarian and breast cancer cells.* Biochem J, 1995. **309 (Pt 3)**: p. 933-40.
105. Xu, Y., et al., *Characterization of an ovarian cancer activating factor in ascites from ovarian cancer patients.* Clin Cancer Res, 1995. **1**(10): p. 1223-32.
106. Murph, M.M., et al., *Lysophosphatidic acid decreases the nuclear localization and cellular abundance of the p53 tumor suppressor in A549 lung carcinoma cells.* Mol Cancer Res, 2007. **5**(11): p. 1201-11.
107. Pustilnik, T.B., et al., *Lysophosphatidic acid induces urokinase secretion by ovarian cancer cells.* Clin Cancer Res, 1999. **5**(11): p. 3704-10.
108. Fishman, D.A., et al., *Lysophosphatidic acid promotes matrix metalloproteinase (MMP) activation and MMP-dependent invasion in ovarian cancer cells.* Cancer Res, 2001. **61**(7): p. 3194-9.
109. Symowicz, J., et al., *Cyclooxygenase-2 functions as a downstream mediator of lysophosphatidic acid to promote aggressive behavior in ovarian carcinoma cells.* Cancer Res, 2005. **65**(6): p. 2234-42.
110. Yamada, T., et al., *Lysophosphatidic acid (LPA) in malignant ascites stimulates motility of human pancreatic cancer cells through LPA1.* J Biol Chem, 2004. **279**(8): p. 6595-605.
111. Yu, S., et al., *Lysophosphatidic acid receptors determine tumorigenicity and aggressiveness of ovarian cancer cells.* J Natl Cancer Inst, 2008. **100**(22): p. 1630-42.
112. Hope, J.M., et al., *LPA receptor 2 mediates LPA-induced endometrial cancer invasion.* Gynecol Oncol, 2009. **112**(1): p. 215-23.
113. Lin, S., et al., *The absence of LPA2 attenuates tumor formation in an experimental model of colitis-associated cancer.* Gastroenterology, 2009. **136**(5): p. 1711-20.
114. Kitayama, J., et al., *Over-expression of lysophosphatidic acid receptor-2 in human invasive ductal carcinoma.* Breast Cancer Res, 2004. **6**(6): p. R640-6.
115. Sun, B., et al., *Induction of macrophage migration inhibitory factor by lysophosphatidic acid: relevance to tumor growth and angiogenesis.* Int J Mol Med, 2003. **12**(4): p. 633-41.
116. Liu, S., et al., *Expression of autotaxin and lysophosphatidic acid receptors increases mammary tumorigenesis, invasion, and metastases.* Cancer Cell, 2009. **15**(6): p. 539-50.
117. Lacroix, M. and G. Leclercq, *Relevance of breast cancer cell lines as models for breast tumours: an update.* Breast Cancer Res Treat, 2004. **83**(3): p. 249-89.
118. Rae, J.M., et al., *MDA-MB-435 cells are derived from M14 melanoma cells--a loss for breast cancer, but a boon for melanoma research.* Breast Cancer Res Treat, 2007. **104**(1): p. 13-9.
119. Ferguson, C.G., et al., *Fluorogenic phospholipid substrate to detect lysophospholipase D/autotaxin activity.* Org Lett, 2006. **8**(10): p. 2023-6.

120. Sliva, D., et al., *Enhancement of the migration of metastatic human breast cancer cells by phosphatidic acid.* Biochem Biophys Res Commun, 2000. **268**(2): p. 471-9.
121. Koike, S., et al., *The N-terminal hydrophobic sequence of autotaxin (ENPP2) functions as a signal peptide.* Genes Cells, 2006. **11**(2): p. 133-42.
122. Gaetano, C.G., et al., *Inhibition of autotaxin production or activity blocks lysophosphatidylcholine-induced migration of human breast cancer and melanoma cells.* Mol Carcinog, 2009.
123. Lee, S. and K.R. Lynch, *Brown recluse spider (Loxosceles reclusa) venom phospholipase D (PLD) generates lysophosphatidic acid (LPA).* Biochem J, 2005. **391**(Pt 2): p. 317-23.
124. Wang, F.M., et al., *SHP-2 promoting migration and metastasis of MCF-7 with loss of E-cadherin, dephosphorylation of FAK and secretion of MMP-9 induced by IL-1beta in vivo and in vitro.* Breast Cancer Res Treat, 2005. **89**(1): p. 5-14.
125. Samadi, N., et al., *Autotaxin protects MCF-7 breast cancer and MDA-MB-435 melanoma cells against Taxol-induced apoptosis.* Oncogene, 2009. **28**: p. 1028-1039.
126. Ferry, G., et al., *S32826, a nanomolar inhibitor of autotaxin: discovery, synthesis and applications as a pharmacological tool.* J Pharmacol Exp Ther, 2008. **327**(3): p. 809-19.
127. Kim, K.S., et al., *GPR4 plays a critical role in endothelial cell function and mediates the effects of sphingosylphosphorylcholine.* Faseb J, 2005. **19**(7): p. 819-21.

APPENDIX

A published version of this thesis has been attached:

Gaetano, C.G., et al., *Inhibition of autotaxin production or activity blocks lysophosphatidylcholine-induced migration of human breast cancer and melanoma cells.* Mol Carcinog, 2009. **48**(9): p. 801-809.

MOLECULAR CARCINOGENESIS 48:801–809 (2009)

Inhibition of Autotaxin Production or Activity Blocks Lysophosphatidylcholine-Induced Migration of Human Breast Cancer and Melanoma Cells

Cristoforo G. Gaetano,[1] Nasser Samadi,[2] Jose L. Tomsig,[3] Timothy L. Macdonald,[4] Kevin R. Lynch,[3] and David N. Brindley[1]*

[1]*Department of Biochemistry, Signal Transduction Research Group, University of Alberta, Edmonton, Alberta, Canada*
[2]*Laboratory Medicine and Pathology, Signal Transduction Research Group, University of Alberta, Edmonton, Alberta, Canada*
[3]*Department of Pharmacology, University of Virginia, Charlottesville, Virginia*
[4]*Department of Chemistry, University of Virginia, Charlottesville, Virginia*

Increased expression of autotaxin in tumors including glioblastoma, breast, renal, ovarian, lung, and thyroid cancers is associated with increased tumor aggressiveness. Autotaxin promotes metastasis as well as cell growth, survival, and migration of cancer cells. These actions could depend on the noncatalytic effects of autotaxin on cell adhesion, or the catalytic activity of autotaxin, which converts lysophosphatidylcholine into lysophosphatidate in the extracellular fluid surrounding the tumor. Both lysophosphatidylcholine (LPC) and lysophosphatidate have been reported to stimulate migration through their respective G-protein coupled receptors. The present study determines the roles of autotaxin, LPC, and lysophosphatidate in controlling the migration of two cancer cell lines: MDA-MB-231 breast cancer cells, which produce little autotaxin and MDA-MB-435 melanoma cells that secrete significant levels of autotaxin. LPC alone was unable to stimulate the migration of either cell type unless autotaxin was present. Knocking down autotaxin secretion, or inhibiting its catalytic activity, blocked cell migration by preventing lysophosphatidate production and the subsequent activation of $LPA_{1/3}$ receptors. We conclude that inhibiting autotaxin production or activity could provide a beneficial adjuvant to chemotherapy for preventing tumor growth and metastasis in patients with high autotaxin expression in their tumors.

Key words: chemotherapy; lysophosphatidate; lysophosphatidylcholine; metastasis

INTRODUCTION

The ability of cancer cells to migrate and invade surrounding tissues is the main determinant of whether metastases will develop. Most aggressive cancers will metastasize and this results in a poorer prognosis for patients requiring treatment. The ability to prevent the formation of metastases after surgical intervention or chemotherapy would provide a powerful tool in decreasing the morbidity and mortality associated with cancer.

Autotaxin (ATX) is a secreted glycoprotein whose level of expression within tumors correlates strongly with their aggressiveness and invasiveness [1]. ATX was first identified in human melanoma A2058 cells [2] and it has also been detected in several other tumor cell lines [3–6]. ATX expression in breast and other cancers is strongly associated with tumor cell survival, growth, migration, invasion, and metastasis [1,7–11]. However, the mechanisms by which ATX modifies cell signaling within the tumor to stimulate angiogenesis, cancer cell migration and metastasis are still not fully understood. A noncatalytic effect of ATX was shown to occur in oligodendrocytes where ATX acts on adhesion through integrin-dependent focal adhesion assembly [12,13]. ATX may thus regulate cell to extracellular matrix interactions that could be linked to cancer aggressiveness. Another mechanism of ATX action is through the conversion of extracellular lysophosphatidylcholine (LPC) to lysophosphatidate (LPA) [14,15], which could change the balance of cell activation by LPC versus LPA.

LPC is an abundant extracellular lipid that is found at up to 200 μM in the circulation [16]. It is produced by the liver, which secretes mainly

Abbreviations: ATX, autotaxin; LPC, lysophosphatidylcholine; LPA, lysophosphatidate; GPR4, G protein-coupled receptor-4; GAPDH, glyceraldehyde phosphate dehydrogenase; FBS, fetal bovine serum; siCTRL, siControl.

*Correspondence to: Department of Biochemistry (Signal Transduction Research Group), University of Alberta, Edmonton, Alberta, Canada T6G 2S2.

Received 18 November 2008; Revised 23 December 2008; Accepted 3 January 2009

DOI 10.1002/mc.20524

Published online 9 February 2009 in Wiley InterScience (www.interscience.wiley.com)

polyunsaturated LPC [16]. Alternatively, mainly saturated LPC is produced by lecithin/cholesterol acyltransferase, which circulates in high-density lipoproteins [17]. It has been proposed that LPC stimulates cell signaling and cell migration through acting as an extracellular ligand for G2A (G_2 accumulation) and G protein-coupled receptor-4 (GPR4) receptors [18–23]. Alternatively, LPC can signal after its conversion to LPA by ATX [7,14].

LPA is a potent signaling molecule that stimulates cell proliferation, neurite retraction, chemotaxis, and wound healing [24,25]. These effects are mediated by at least six G-protein coupled receptors on the cell surface: LPA_1/EDG2, LPA_2/EDG4, LPA_3/EDG7, LPA_4/GPR23/p2y9, LPA_5/GRP92, and LPA_6/p2y5 [26–28]. The expression of these LPA receptors is cell-specific, and each can elicit different responses upon LPA binding. Initial evidence that LPA can be involved in carcinogenesis came from the identification of its role as an activating factor in ovarian cancer. LPA is present in high concentrations in the ascites fluid of ovarian tumors and it stimulates cell proliferation and metastasis [29,30]. These actions are mediated mainly through LPA_1 and LPA_3 receptors [11,31–33]. LPA stimulates angiogenesis by elevating levels of vascular endothelial growth factor [8]. LPA also increases the synthesis of macrophage migration inhibitory factor, a tumor promoter, in a colon cancer line [34] and it decreases the expression of the tumor suppressor, p53, in lung cancer cells [35].

Two main pathways have been identified for LPA production of extracellular LPA [36]. During inflammation, secretory PLA_2 is produced, which generates LPA from phosphatidate on exposed membranes [37]. The second, and more significant source of extracellular LPA, is through the action of ATX on extracellular LPC [14].

In the present work, we examined the effects of LPC and LPA on the migration of MDA-MB-231 breast cancer cells, which produce very little ATX, and MDA-MB-435 melanoma cells [38], which secrete abundant ATX. We found that MDA-MB-231 cells migrate in response to LPC only if ATX is present. Also, knocking down ATX expression in MDA-MB-435 cells, or inhibiting the catalytic action of ATX, blocked cell migration in the presence of LPC, but not LPA. We propose that inhibiting the production, or activity of ATX could decrease new tumor growth and metastasis following surgical excision of a tumor given that LPC is abundant in the environment of malignant tumors and it can readily be converted to LPA by tumor-derived ATX.

MATERIALS AND METHODS

Materials

Mouse anti-glyceraldehyde 3-phospate dehydrogenase (GAPDH) was from Sigma–Aldrich (Oakville, ON, Canada). Rabbit anti-ATX and recombinant ATX were gifts from Dr. T. Clair (National Cancer Institute, Bethesda, MA). Secondary antibodies were: AlexaFluor© 680 goat anti-mouse IgG, A-21057 was from Invitrogen Life Technologies (Carlsbad, CA); IRDye 800 goat anti-rabbit IgG (Rockland Immunochemicals, Philadelphia, PA). VPC32183 was purchased from Avanti Polar Lipids (Alabaster, AL). Oleoyl-L-α-lysophosphatidic acid, sodium salt (LPA), oleoyl-L-α-LPC, fatty acid-free bovine serum albumin, activated charcoal (Norit®), Hoechst 33258, horseradish peroxidase, choline oxidase, 4-aminoantipyrine, N-ethyl-N-(2-hydroxy-3-sulfopropyl)-m-toluidine and fibronectin were purchased from Sigma–Aldrich (Oakville, ON, Canada and St. Louis, MO). Fetal bovine serum (FBS) was from Medicorp, Inc. (Montréal, PQ, Canada). The ATX inhibitors, VPC8a202 and S32826 were synthesized as described previously [39,40]. Transwells® (polycarbonate, 13 mm D, 12 μm pore size) were obtained from Corning (Corning, NY). On the day before the migration assays they were coated with 120 μL of 0.15 mg/mL fibronectin and allowed to dry.

Cell Culture

MDA-MB-435 and MDA-MB-231 cells were obtained from the American Type Culture Collection. The cells were cultured in RPMI 1640 medium (GIBCO, Burlington, ON, Canada) supplemented with 10% FBS and an antibiotic/antimycotic cocktail (penicillin, streptomycin, amphotericin B) (Invitrogen Life Technologies) at 5% CO_2, 95% humidity and 37°C.

Collection and Concentration of Conditioned Media

Equal numbers of cells were plated onto 10 cm dishes and they were grown until 90% confluence. Dishes were washed and then 10 mL of RPMI 1640 containing 0.1% BSA (≥96% fatty acid free) was added. After 24 h cells were washed and 10 mL of RPMI 1640 was added. The dishes were incubated for a further 24 h, the conditioned media was collected and cells on each dish were counted. Collected conditioned media were then centrifuged at $1{,}500 \times g$ for 10 min to remove whole cells and debris and they was then stored at −20°C. Conditioned media were concentrated approximately 20- to 30-fold using Centricon® YM-10 centrifugal filter devices (Millipore, Billerica, MA). Filters were prerinsed with 2 mL of water to remove glycerine and samples were centrifuged at 5,000*g* for 120 min, or until the desired final volume was obtained. Filters were then inverted and centrifuged at 1,500*g* for 2 min to collect concentrated media. The final volume was determined by weighing.

mRNA Expression

Total RNA was extracted from cell lysates using the RNAqueous kit (Ambion, Streetsville, ON,

Canada) according the manufacturer's instruction. Extracted RNA was treated with DNAase (DNA-free kit, Ambion). RNA reverse transcription reaction was performed with Superscript II reverse transcriptase (Invitrogen Life Technologies) in the presence of random primers according to the manufacturer's instructions. A control reaction without reverse transcriptase was performed in parallel to detect genomic DNA contamination. cDNA was calculated assuming 100% conversion from RNA. Real time-RT-PCR was performed by mixing 25 μL of master mix containing 2 × SYBR Green buffer mix and forward and reverse primers (Invitrogen Life Technologies) to a 3.5 μL of sample of cDNA in 96 well plates. A 316 bp fragment of the constitutively expressed housekeeping human GAPDH was used to normalize the expression of ATX mRNA. Primers for human ATX were: sense, 5′-ACAACGAGGAGAGCTGCAAT-3′, and anti-sense, 5′-AGAAGTCCAGGCTGGTGAGA-3′. Primers for human GAPDH were: sense, 5′-ACAGTCAGCCGCATCTTCTT-3′ and antisense, 5′-GACAAGCTTCCCGTTCTCAG-3′. Samples of cDNA were assayed in triplicates on the 7500 Real Time PCR System (Applied Biosystems, Streetsville, ON, Canada). The transcript number of human GAPDH was quantified, and each sample was normalized on the basis of GAPDH mRNA content.

Boyden Chamber Assay for Migration

Two million cells were seeded in a 25 cm^2 flask with growth medium for at least 48 h. Starvation medium (RPMI 1640 containing 0.1% BSA, ≥96% fatty acid free) was added for the last 18 h before the migration experiment. Cells were washed twice with HBS, trypsinized, and collected in starvation media and then 1 mL of 0.1% trypsin inhibitor solution in HBS was added. Cells were centrifuged down, media were removed by aspiration, and cells were resuspended in starvation media and counted. Cells (300 000) were seeded into each of the fibronectin coated Transwell® filters and incubated for 45 min for attachment. Filters were then transferred into bottom chambers that contained 1.5 mL of starvation medium with 0.2% charcoal-treated FBS (FBS-C) and various agonists. This charcoal treatment removed >95% of the LPA as assessed after spiking the FBS with ^{32}P-labeled LPA. This means that the concentration of LPA added in the diluted serum should have been <1 nM. Chambers were incubated at 37°C and cells were allowed to migrate through the pores in the filter for 3 or 6 h. The basal level of migration was measured with 0.2% FBS-C in the bottom chamber and 5% FBS was used as a positive control for stimulated migration. After migration, cells were then fixed in 5% formaldehyde for 1 h, or overnight. Filters were then rinsed in water and placed in 1 μg/mL Hoechst 33258 stain for 2 h. Then the upper surface of the filters was cleaned with a moist cotton swab to remove cells that had not migrated. Filters were washed again and placed in PBS. Four to six random fields were photographed under a Leica DM IRB fluorescence microscope at 40× magnification without knowing the treatment and the average numbers of cells per field was calculated.

Western Blot Analysis

Concentrated conditioned media were analyzed by SDS–PAGE according to Laemmli [41]. Proteins were transferred at 450 mA for 5 h onto nitrocellulose membranes (Trans-Blot® Transfer Medium, Bio-Rad, Mississauga, ON, Canada) in transfer buffer (192 mM glycine, 24 mM Tris base, pH 8.5 and 20% (v/v) ethanol). Membranes were blocked in 50% PBS and 50% Odyssey™ blocking buffer (Li-Cor Biosciences, Lincoln, NE) for a minimum of 1.5 h. All antibodies were diluted in 50:50 PBS/Odyssey™ blocking buffer with 0.1% (v/v) Tween-20. Membranes were incubated with anti-ATX (rabbit, 1:10 000) for 1 h. Membranes were then washed four times with PBS containing 0.1% Tween-20 and incubated in IRDye 800 goat anti-rabbit IgG (Rockland Immunochemicals, 1:10 000) for 1 h and washed three times in wash buffer and once in PBS alone. Membranes were scanned using the Odyssey™ Imager (Li-Cor).

Autotaxin Activity Assay

The assay of ATX activity in cells was based on the method described by Ferguson et al. [42] using a fluorogenic phospholipid ATX substrate, FS-3 (Echelon Biosciences, Salt Lake City, UT). FS-3 was diluted to 3.1 μM in a solution containing: 140 mM NaCl, 5 mM KCl, 1 mM $CaCl_2$, 1 mM $MgCl_2$, 50 mM Tris–HCl, pH 8.0, and 1 mg/mL BSA. The solution was heated at 60°C for 10 min to destroy any enzymatic activity in the BSA and then cooled to 37°C before use. Forty microliters of FS-3 solution was added to 10 μL of cell lysate, or concentrated conditioned media in a black-wall, clear-bottom 96 well Costar® half-area plate. Measurements were then taken at appropriate intervals using a Fluoroskan Ascent fluorometer (Thermo Lab Systems, Gormley, ON, Canada) at an excitation wavelength of 485 nm and an emission wavelength of 527 nm.

For the kinetic studies, human recombinant ATX was subcloned into the mammalian expression vector cDNA3.1/V5His-TOPO (Invitrogen Life Technologies) and expressed as a C-terminus V5- and 6xHis-tagged protein in HEK-293 cells using PolyFect® (Qiagen, Germantown, MD) as a transfection reagent. ATX was purified from the culture medium using a nickel-Sepharose resin (Qiagen) according to manufacturer's instructions and the buffer was changed to PBS using 30 kDa cutoff Centricon tubes (Millipore). ATX DNA was generated from an EST I.M.A.G.E. clone 5174518 using the following forward and reverse primers 5′-CGC GCT AGC ATG GCA AGG AGG AGC TCG TTC-3′; 5′-AAT CTC GCT

CTC ATA TGT ATG CAG-3′ to amplify the ATX ORF. ATX activity was measured essentially as described by Umezu-Goto et al. [7] by determining the release of choline after incubation at 37°C for 18 h in 100 μL of a buffer consisting of 100 mM Tris–HCl, pH 9.0, 500 mM NaCl, 5 mM $MgCl_2$, 30 μM $CoCl_2$, 0.05% Triton X-100, 0.5 μM VPC8a202 and various concentrations of oleoyl-LPC (Avanti Polar Lipids). Choline was detected colorimetrically at 555 nm after adding 100 μL of 50 mM Tris–HCl, pH 8.0, 5 mM $MgCl_2$, 50 U/mL horseradish peroxidase, 18 U/mL choline oxidase, 5 mM 4-aminoantipyrine, and 3 mM N-ethyl-N-(2-hydroxy-3-sulfopropyl)-m-toluidine.

Knockdown of Autotaxin Expression Using siRNA

Knockdown of ATX was achieved using SMARTpool® siRNAs (Dharmacon, Inc., Lafayette, CO). About 800 000 cells were plated on 10 cm dishes with 15 mL of antibiotic-free RPMI 1640 containing 10% FBS. Cells were grown for 2 d until about 50% confluency. Before transfection, the medium was replaced with 7 mL of fresh antibiotic-free media. Ten microliters of stock siRNA (50 μM) was diluted in 1.5 mL of Opti-MEM Reduced Serum Medium (Invitrogen Life Technologies). In a separate tube, 30 μL of Lipofectamine 2000 (Invitrogen Life Technologies) was mixed with 1.5 mL Opti-MEM and incubated at room temperature for 15 min. The siRNA and the Lipofectamine solutions were then combined and incubated for another 15 min at room temperature. Each dish of cells received 3 mL of the siRNA-Lipofectamine 2000 complex that was added drop-wise while swirling the dish. The final concentrations of Lipofectamine 2000 and siRNA were 1.4 μg/mL and 50 nM respectively. Cells were then incubated for 24 h at 37°C and the medium was collected as described above. Cells on each dish were trypsinized and counted so that equivalent amounts of concentrated media could be used in the migration assays.

Statistics

Results are presented as means ± SEM from at least three independent experiments, unless otherwise indicated. Statistical differences were calculated using GraphPad 4 software (Prism) by ANOVA with a Newman–Keuls post-hoc test and paired *t*-tests.

RESULTS

Differential Effects of Lysophosphatidylcholine and Lysophosphatidate on the Migration of MDA-MB-231 Breast Cancer Cells and MDA-MB-435 Melanoma Cells

We first compared the migration of MDA-MB-231 breast cancer cells and MDA-MB-435 cells, which are now known to be derived from M14 melanoma cells [38]. MDA-MB-231 and MDA-MB-435 showed a similar migratory response to LPA over 6 h, with maximum migration occurring with about 0.5 μM LPA. This LPA concentration elicited a migratory response similar to that obtained with 5% charcoal treated-FBS (Fig. 1A). MDA-MB-231 cells showed no significant stimulation of migration over the 6 h incubation with any LPC concentration employed (Fig. 1B). By contrast, MDA-MB-435 cells showed a stimulation of migration in response to LPC concentrations of ≥5 μM in the bottom chamber.

ATX Activity Is Required for Lysophosphatidylcholine-Induced Cell Migration

The results in Figure 1 could be explained in two ways. First, the MDA-MB-231 cells may not express putative receptors that respond to LPC, whereas MDA-MB-435 cells express these receptors. Second,

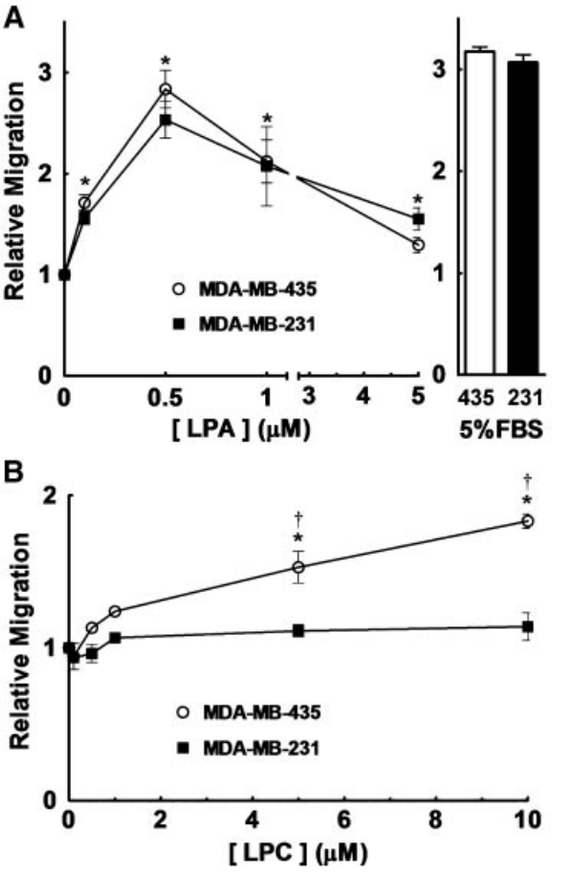

Figure 1. Effects of lysophosphatidate and lysophosphatidylcholine on the migration of MDA-MB-435 and MDA-MB-231 cells. Panel A shows the migration of MDA-MB-435 (○), and MDA-MB-231 (■) cells after a 3 h incubation with different concentrations of LPA. Migration in response to 5% charcoal-stripped FBS was used as a positive control. Panel B shows migration when the cells were incubated for 6 h with different concentrations of LPC. Results are expressed relative to the number of cells migrating with only basal media (RPMI 1640 with 0.1% BSA and 0.2% FBS-C), which was given a value of 1. Typically, basal migration consisted of approximately 75 cells per field for a 3 h incubation and 120 cells per field for a 6 h incubation. Results are means ± SEM from at least three independent experiments. Statistically significant differences between basal migration and agonist-stimulated migration are indicated by $*P < 0.01$ and between cell lines are indicated by $^{\dagger}P < 0.01$.

and more likely, MDA-MB-435 cells could express ATX that produces LPA from LPC, which stimulates cell migration, whereas MDA-MB-231 cells do not express ATX. To test the latter hypothesis, we measured ATX expression in both cells lines. The MDA-MB-435 cells expressed significantly more ($P < 0.05$) ATX mRNA than the MDA-MB-231 cells as shown by real-time RT-PCR analysis (Fig. 2A). Furthermore, concentrated medium from MDA-MB-231 cells showed very low ATX activity compared to MDA-MB-435 medium (Fig. 2B). Western Blot analysis of medium from MDA-MB-435 cells (Fig. 2C) showed marked expression of ATX, which migrated with the recombinant ATX standard at about 100 kDa as expected [7]. MDA-MB-435 cells can, therefore, be used as a convenient source of ATX for future experiments described below. By contrast, ATX was barely detectable in equivalent amounts of medium from MDA-MB-231 cells.

We could not detect any significant ATX activity or protein expression in the lysates from MDA-MB-435 and MDA-MB-231 cells (results not shown), which implies that ATX is mainly a secreted protein as shown previously [14].

Concentrated Medium From MDA-MB-435 Cells Stimulates Cell Migration in the Presence of Lysophosphatidylcholine Because of its Autotaxin Activity

To determine why MDA-MB-435 and MDA-MB-231 cells respond differently to LPC, we measured the effects of adding concentrated media from these cells to the bottom well of the migration chamber. MDA-MB-231 cells show no significant migration in the presence of LPC and their own concentrated medium. By contrast, a migratory response similar to that obtained with 5% charcoal-treated FBS, or 0.5 μM LPA was obtained when concentrated medium from MDA-MB-435 and LPC were added to the bottom chamber. This latter effect was completely abolished by the addition of 1 μM VPC8a202, an ATX inhibitor [39], to the wells (Fig. 3A).

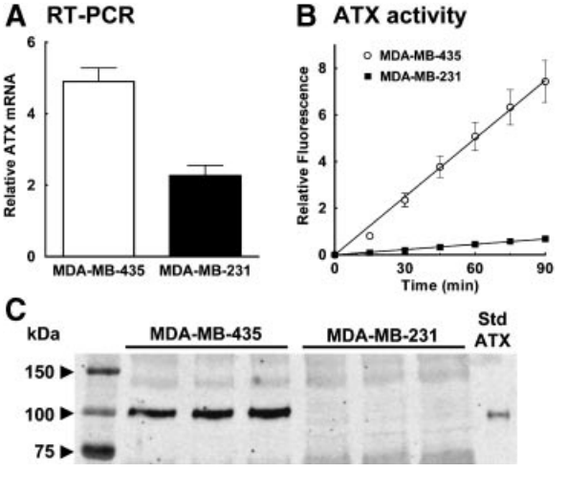

Figure 2. MDA-MB-435 cells secrete significant amounts of active ATX into the extracellular medium compared to MDA-MB-231 cells. Panel A shows the relative mRNA levels of ATX compared to GAPDH in MDA-MB-435 and MDA-MB-231 cells. Results are means ± SEM from at least three independent experiments. Panel B shows the results from the fluorescence assay for ATX activity of concentrated conditioned media collected from MDA-MB-435 (○), or MDA-MB-231 (■) cells. Results are means ± SEM from at least three independent experiments. Panel C shows the Western blot analysis for ATX of concentrated media collected from three separate dishes of MDA-MB-435 or MDA-MB-231 cells. Recombinant ATX from Dr. T. Clair was used as a standard (StdATX).

A similar experiment was performed with MDA-MB-435 cells. Addition of concentrated medium from MDA-MB-231 cells had no significant effect on the migration of MDA-MB-435 cell in the presence, or absence of LPC (Fig. 3B). By contrast, a significant stimulation of migration was observed when concentrated medium from MDA-MB-435 cells was added to the bottom chamber with LPC. This response was completely blocked by the addition of 1 μM of the ATX inhibitor, VPC8a202. We also used 1 μM S32826 ([4-(tetradecanoylamino)-benzyl]-phosphonic acid), another ATX inhibitor [40], and found that it also completely blocked LPC-induced migration of MDA-MB-435 cells (Fig. 3C). As controls for the experiments in Figure 3B and C, we used LPA to stimulate migration through its G-protein coupled receptors. VPC8a202 and S32826 did not significantly affect this LPA-induced stimulation of migration for either cell line (Fig. 3B and C). This demonstrates that neither inhibitor affects migration per se and that the inhibition of migration depends on blocking the conversion of LPC to LPA.

To provide further evidence to support the conclusion that the stimulatory effect of LPC on the migration of MDA-MB-435 and MDA-MB-231 cells depends on the catalytic activity of ATX, we established that VPC8a202 and S32826 inhibited ATX activity under the conditions of the FS-3 fluorescence assay by about 93% and 90%, respectively. We also performed more detailed kinetic studies on the inhibition of ATX activity by VPC8a202 using the natural substrate, LPC. Our results show that VPC8a202 acts mainly as a competitive inhibitor of ATX and that it prevents the conversion of LPC to LPA as expected from a substrate analogue, with a K_i of about 390 nM (Fig. 4). Previous work showed that S32826 is also a nM inhibitor of ATX [40]. Concentrations of VPC8a202 and S32826 in the μM range are, therefore, effective at inhibiting ATX and this supports our interpretation that the observed migratory effects of LPC reflect the conversion of LPC to LPA by ATX.

To further validate the results with the ATX inhibitors on migration, we also knocked down ATX expression in MDA-MB-435 cells using siRNA. Conditioned media from siATX treated cells showed an 85% decrease in ATX activity compared to the siControl (siCTRL) treated cells (Fig. 5A).

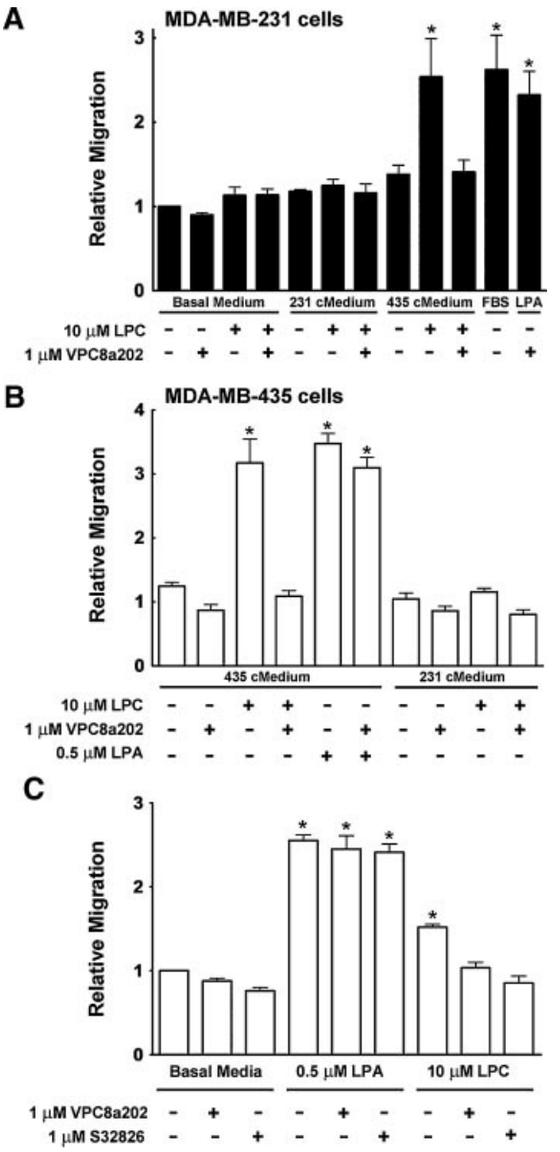

Figure 3. Stimulation of migration by lysophosphatidylcholine depends on autotaxin activity. Panel A shows the migration of MDA-MB-231 cells over 3 h in the presence of basal medium or concentrated medium prepared from either MDA-MB-231 cells (231 cMedium), or from MDA-MB-435 cells (435 cMedium). These experiments were performed in the presence or absence of 10 μM LPC, or 1 μM of the ATX inhibitor, VPC8a202. Migration of MDA-MB-231 cells with only basal media (RPMI 1640 with 0.1% BSA and 0.2% FBS) present was given a value of 1. Migrations in the presence of 5% FBS and 0.5 μM LPA plus VPC8a202 were used as controls. Panel B shows results from similar experiments using MDA-MB-435 cells over a 3 h period. Panel C shows the effects of the ATX inhibitors, VPC8a202 and S32826, on the migration of MDA-MB-435 cells over 3 h in the absence of concentrated medium. Results are means ± SEM from at least three independent experiments. Statistically significant differences are indicated by $*P < 0.01$.

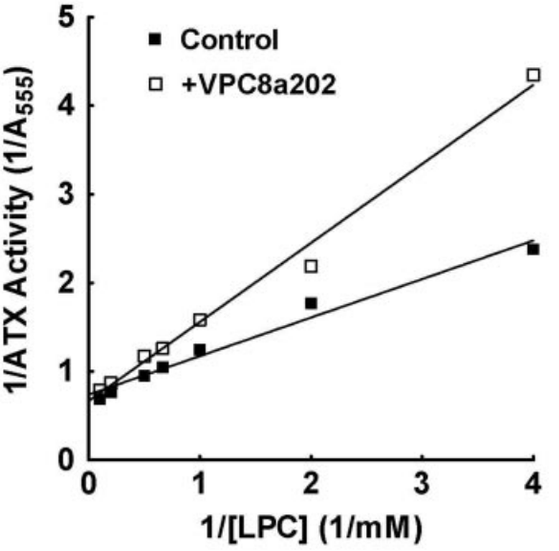

Figure 4. Kinetics of inhibition of ATX activity by VPC8a202. The initial rate of recombinant ATX activity was measured colorimetrically at different concentrations of LPC in presence and absence of 0.5 μM VPC8a202. Activity was expressed as the release of choline during 18 h and it is represented by the absorbance of the product at 555 nm (A555). Each point is the average of three measurements (SD values for the reaction rates were less than 5% of every measurement and are not depicted). Consumed substrate was less than 10% in every case thus ensuring an initial rate of reaction. Results were fitted to a straight line by linear regression. The apparent K_m for LPC was about 588 μM.

Furthermore, expression of the ATX protein in conditioned media from siATX treated cells was markedly reduced to levels that were undetectable by Western blotting (Fig. 5B).

There was no stimulation of the migration of MDA-MB-435 cells when we added only concentrated media from cells treated with siATX, or siCTRL. By contrast, addition of LPC to concentrated medium from cells treated with the siCTRL elicited a migratory response (Fig. 5C), but this stimulation was not observed when ATX formation was blocked with siATX.

We also tested the migration of MDA-MB-435 when exposed to LPC, or LPA directly, but using a 6 h incubation for the migration assay. The siCTRL and the siATX treated cells migrated to the same extent in the absence of agonist. Addition of 10 μM LPC stimulated the migration of siCTRL treated cells, but not siATX-treated cells. As a control, we showed that the siATX treated cells still showed a normal migration with 0.5 μM LPA. The results emphasize that the cells treated with siATX were not migration deficient. They we able to respond normally to LPA, but they were unable to migrate to LPC because of the ATX knockdown (Fig. 6).

These results establish that the LPC effect in stimulating cell migration is dependent on the catalytic activity of ATX and LPA production, which could then stimulate migration through LPA receptors. This is confirmed in Figure 7 where 1 μM VPC32183, an $LPA_{1/3}$ receptor antagonist [43], was added to the concentrated medium from MDA-MB-

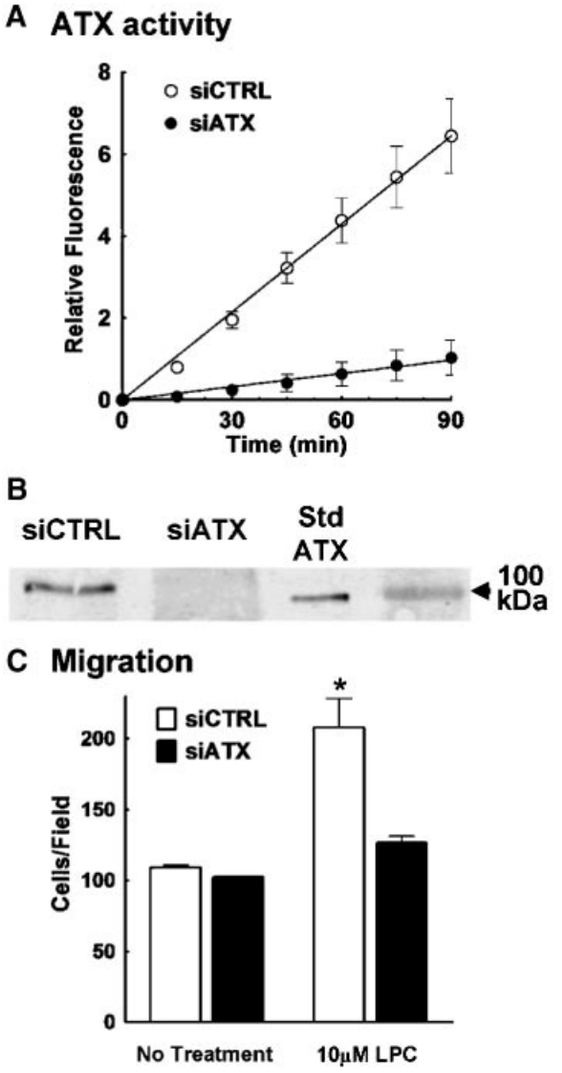

Figure 5. Knock-down of ATX with siRNA significantly decreases the migratory potential of concentrated medium from MDA-MB-435 cells. Concentrated medium was collected from three dishes of MDA-MB-435 cells treated with siRNA for ATX (siATX) and three dishes treated with control siRNA (siCTRL). Panel A shows a fluorescence assay representing ATX activity in siCTRL concentrated medium (○) and in siATX concentrated medium (●). Error bars indicate the SEM of three experimental values. Panel B shows the Western blot analysis of a representative sample of concentrated media that were probed for ATX. Recombinant ATX was used as a standard (StdATX). Panel C compares the migration of MDA-MB-435 cells over a 3 h incubation in the presence or absence of LPC and concentrated medium collected from MDA-MB-435 cells that were treated with siCTRL (white bars) or siATX (dark bars). Results are means ± SEM from three independent experiments. Statistically significant differences are indicated by $*P < 0.01$.

435 cells. VPC32183 inhibited LPC-induced migration in the presence of concentrated medium, demonstrating that the effect of LPC depends on its conversion to LPA. As a control, we also showed that VPC32183 inhibited migration when LPA was added

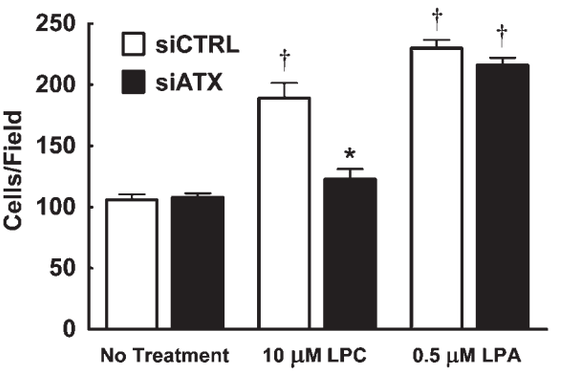

Figure 6. Knockdown of ATX with siRNA in MDA-MB-435 cells abolishes stimulation of migration by lysophosphatidylcholine. A 6 h incubation was used to measure the migration of MDA-MB-435 cells that were treated with siATX or siCTRL. Migration in basal media (RPMI 1640 with 0.1% BSA and 0.2% FBS-C) was compared to migration in the presence of 10 μM LPC, or 0.5 μM LPA. Results are means ± SEM from four independent experiments. Statistically significant differences between alternate siRNA treated cells are indicated by $*P < 0.01$ and between treatments compared to control are indicated by $^{\dagger}P < 0.01$.

directly. There was also a small inhibitory effect of VPC32183 when neither LPC nor LPA was added, which probably resulted from the presence of some secreted LPC or LPA in the concentrated medium from the MDA-MB-435 cells.

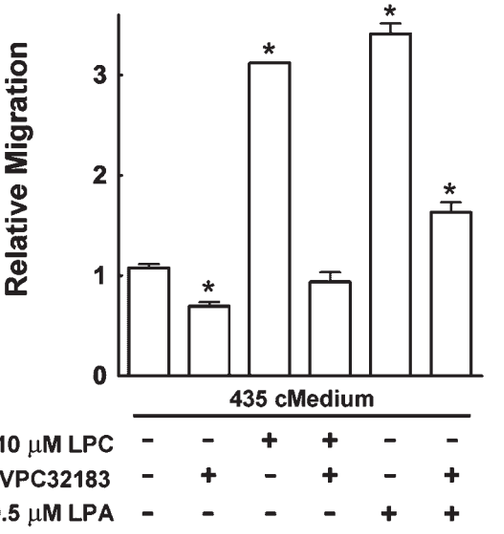

Figure 7. The LPA receptor antagonist, VPC32183, inhibits migration of MDA-MB-435 cells. A 3 h incubation was used to measure the migration of MDA-MB-435 cells in the presence of their own concentrated medium with either LPC or LPA, and in the presence or absence of the $LPA_{1/3}$ receptor antagonist, VPC32183. Migration in the presence of agonists/antagonists was compared to the number of cells migrating in basal media (RPMI 1640 with 0.1% BSA and 0.2% FBS-C), which is given a value of 1. Results are means ± SEM from at least three independent experiments. Statistically significant differences compared to the untreated control are indicated by $*P < 0.01$.

DISCUSSION

Increased ATX expression in tumors such as glioblastoma, lung, breast, renal, ovarian, and thyroid cancers is correlated with their aggressiveness [6–10,24]. In this article, we investigated the mechanisms for this local effect of ATX by studying the migration of MDA-MB-435 melanoma cells and MDA-MB-231 breast cancer cells. These cells are both able to migrate well in response to serum, or LPA. We found that MDA-MB-435 cells secrete abundant ATX, whereas ATX secretion from MDA-MB-231 was barely detectable. Significantly, MDA-MB-435 cells migrated in response to LPC, whereas MDA-MB-231 did not. We, therefore, hypothesized that LPC does not induce migration of these cells per se, but rather its effects depend on its conversion to LPA by ATX. Therefore, decreased expression or inhibition of ATX should diminish the LPC response.

We verified this hypothesis as follows: (a) addition of medium from MDA-MB-435, but not from MDA-MB-231 cells, enabled MDA-MB-231 cells to migrate in response to LPC; (b) this effect was abolished by the suppression of ATX expression using siRNA for ATX, (c) inhibition of ATX activity with two different ATX inhibitors, VPC8a202 and S32826, completely blocked the stimulatory effect of LPC on migration and (d) LPC-induced migration was inhibited by an $LPA_{1/3}$ receptor antagonist, VPC32183. These results establish that the major action of ATX on migration in MDA-MB-435 and MDA-MB-231 cells in this system is through the conversion of LPC to LPA. However, we cannot rule out that ATX could exert a noncatalytically action on migration in vivo through its C-terminal region, which can modify cell adhesion.

Although LPC has been widely described to stimulate cell activation and migration directly through its putative action on G2A and GPR4 receptors [18], much of this work is now in question. G2A and GPR4 are now considered to be proton-sensing receptors whose response is negatively regulated by LPC [44,45]. We found no evidence that the zwitterionic lipid, LPC, is able to stimulate migration. Rather its action depends on conversion to the acidic lipid, LPA, by ATX. This conclusion is also supported by two very recent publications. First, independent work shows that small molecule inhibitors of ATX block melanoma cell migration and invasion [46]. Secondly, we showed that ATX activity is required for LPC to protect MCF-7 breast cancer and MDA-MB-435 melanoma cells against Taxol-induced apoptosis [47].

LPC is present in blood and extracellular fluids at concentrations up to 200 μM. Secretion of ATX into the blood or the interstitial fluid surrounding a tumor can convert the relatively abundant LPC, which does not stimulate migration, into the potent bioactive modulator, LPA. This lipid provides a survival signal for cancer cells and it causes them to migrate and metastasize. This is consistent with the fact that high levels of ATX are often found in aggressive cancers. Our work demonstrates that inhibition of ATX expression, or blocking its catalytic activity, could provide very powerful tools to improve the efficacy of surgery and chemotherapy in the treatment of metastatic disease in patients where ATX expression is high. It is, therefore, hoped that our work will lead to the development of ATX inhibitors that can be used therapeutically as an adjuvant in the treatment of cancer.

ACKNOWLEDGMENTS

We thank Mr. J. Dewald for excellent technical assistance, and Dr. F. Bamforth and Dr. G.S. Cembrowski for their support of this study. We also thank Dr. T. Clair for providing recombinant ATX and the ATX antibody and Dr. J.A. Boutin (Institut de Recherches Servier) for supplying S32826. DNB is a recipient of a Medical Scientist Award from the Alberta Heritage Foundation for Medical Research. NS is a recipient of scholarships from Iranian Ministry of Health and the Bell McLeod Educational Fund from Department of Laboratory Medicine and Pathology, University of Alberta. This work was supported by grants to DNB from the Canadian Institute of Health Research (MOP 81137) and from NIH (R01 GM052722) to KRL. The provision of recombinant ATX and ATX antibody through Dr. T. Clair was made possible by the Intramural Research Program of the NIH, National Cancer Institute, Center for Cancer Research.

REFERENCES

1. Yang SY, Lee J, Park CG, et al. Expression of autotaxin (NPP-2) is closely linked to invasiveness of breast cancer cells. Clin Exp Metastasis 2002;19:603–608.
2. Stracke ML, Krutzsch HC, Unsworth EJ, et al. Identification, purification, and partial sequence analysis of autotaxin, a novel motility-stimulating protein. J Biol Chem 1992;267: 2524–2529.
3. Kishi Y, Okudaira S, Tanaka M, et al. Autotaxin is overexpressed in glioblastoma multiforme and contributes to cell motility of glioblastoma by converting lysophosphatidylcholine to lysophosphatidic acid. J Biol Chem 2006;281:17492–17500.
4. Euer N, Schwirzke M, Evtimova V, et al. Identification of genes associated with metastasis of mammary carcinoma in metastatic versus non-metastatic cell lines. Anticancer Res 2002;22:733–740.
5. Stassar MJ, Devitt G, Brosius M, et al. Identification of human renal cell carcinoma associated genes by suppression subtractive hybridization. Br J Cancer 2001;85:1372–1382.
6. Kehlen A, Englert N, Seifert A, et al. Expression, regulation and function of autotaxin in thyroid carcinomas. Int J Cancer 2004;109:833–838.
7. Umezu-Goto M, Kishi Y, Taira A, et al. Autotaxin has lysophospholipase D activity leading to tumor cell growth and motility by lysophosphatidic acid production. J Cell Biol 2002;158:227–233.
8. So J, Wang FQ, Navari J, Schreher J, Fishman DA. LPA-induced epithelial ovarian cancer (EOC) in vitro invasion and

migration are mediated by VEGF receptor-2 (VEGF-R2). Gynecol Oncol 2005;97:870–878.
9. Nam SW, Clair T, Campo CK, Lee HY, Liotta LA, Stracke ML. Autotaxin (ATX), a potent tumor motogen, augments invasive and metastatic potential of ras-transformed cells. Oncogene 2000;19:241–247.
10. Nam SW, Clair T, Kim YS, et al. Autotaxin (NPP-2), a metastasis-enhancing motogen, is an angiogenic factor. Cancer Res 2001;61:6938–6944.
11. Hama K, Aoki J, Fukaya M, et al. Lysophosphatidic acid and autotaxin stimulate cell motility of neoplastic and non-neoplastic cells through LPA1. J Biol Chem 2004;279: 17634–17639.
12. Fox MA, Alexander JK, Afshari FS, Colello RJ, Fuss B. Phosphodiesterase-I alpha/autotaxin controls cytoskeletal organization and FAK phosphorylation during myelination. Mol Cell Neurosci 2004;27:140–150.
13. Dennis J, Nogaroli L, Fuss B. Phosphodiesterase-Ialpha/autotaxin (PD-Ialpha/ATX): A multifunctional protein involved in central nervous system development and disease. J Neurosci Res 2005;82(6) 737–742.
14. Tokumura A, Majima E, Kariya Y, et al. Identification of human plasma lysophospholipase D, a lysophosphatidic acid-producing enzyme, as autotaxin, a multifunctional phosphodiesterase. J Biol Chem 2002;277:39436–39442.
15. Baker DL, Fujiwara Y, Pigg KR, et al. Carba analogs of cyclic phosphatidic acid are selective inhibitors of autotaxin and cancer cell invasion and metastasis. J Biol Chem 2006;281: 22786–22793.
16. Brindley DN. Hepatic secretion of lysphosphatidylcholine: A novel transport system for polyunsaturated fatty acids and choline. J Nutr Biochem 1993;4:442–449.
17. Aoki J, Taira A, Takanezawa Y, et al. Serum lysophosphatidic acid is produced through diverse phospholipase pathways. J Biol Chem 2002;77:48737–48744.
18. Radu CG, Yang LV, Riedinger M, Au M, Witte ON. T cell chemotaxis to lysophosphatidylcholine through the G2A receptor. Proc Natl Acad Sci USA 2004;101:245–250.
19. Kim KS, Ren J, Jiang Y, et al. GPR4 plays a critical role in endothelial cell function and mediates the effects of sphingosylphosphorylcholine. FASEB J 2005;9:819–821.
20. Zhu K, Baudhuin LM, Hong G, et al. Sphingosylphosphorylcholine and lysophosphatidylcholine are ligands for the G protein-coupled receptor GPR4. J Biol Chem 2001;76: 41325–41335.
21. Rikitake Y, Hirata K, Yamashita T, et al. Expression of G2A, a receptor for lysophosphatidylcholine, by macrophages in murine, rabbit, and human atherosclerotic plaques. Arterioscler Thromb Vasc Biol 2002;2:2049–2053.
22. Kabarowski JH, Zhu K, Le LQ, Witte ON, Xu Y. Lysophosphatidylcholine as a ligand for the immunoregulatory receptor G2A. Science 2001;93:702–705.
23. Lin P, Ye RD. The lysophospholipid receptor G2A activates a specific combination of G proteins and promotes apoptosis. J Biol Chem 2003;78:14379–14386.
24. Mills GB, Moolenaar WH. The emerging role of lysophosphatidic acid in cancer. Nat Rev Cancer 2003;3:582–591.
25. Brindley DN. Lipid phosphate phosphatases and related proteins: signaling functions in development, cell division, and cancer. J Cell Biochem 2004;92:900–912.
26. Lynch KR. Lysophospholipid receptor nomenclature. Biochim Biophys Acta 2002;1582:70–71.
27. Lee CW, Rivera R, Gardell S, Dubin AE, Chun J. GPR92 as a new G12/13- and Gq-coupled lysophosphatidic acid receptor that increases camp, LPA5. J Biol Chem 2006;281: 23589–23597.
28. Pasternack SM, von Kugelgen I, Aboud KA, et al. G protein-coupled receptor P2Y5 and its ligand LPA are involved in maintenance of human hair growth. Nat Genet 2008;40: 329–334.
29. Xu Y, Fang XJ, Casey G, Mills GB. Lysophospholipids activate ovarian and breast cancer cells. Biochem J 1995;309:933–940.
30. Xu Y, Gaudette DC, Boynton JD, et al. Characterization of an ovarian cancer activating factor in ascites from ovarian cancer patients. Clin Cancer Res 1995;1:1223–1232.
31. Van Leeuwen FN, Olivo C, Grivell S, Giepmans BN, Collard JG, Moolenaar WH. Rac activation by lysophosphatidic acid LPA1 receptors through the guanine nucleotide exchange factor Tiam1. J Biol Chem 2003;278:400–406.
32. Shida D, Kitayama J, Yamaguchi H, et al. Lysophosphatidic acid (LPA) enhances the metastatic potential of human colon carcinoma DLD1 cells through LPA1. Cancer Res 2003;63: 1706–1711.
33. Yamada T, Sato K, Komachi M, et al. Lysophosphatidic acid (LPA) in malignant ascites stimulates motility of human pancreatic cancer cells through LPA1. J Biol Chem 2004;279: 6595–6605.
34. Sun B, Nishihira J, Suzuki M, et al. Induction of macrophage migration inhibitory factor by lysophosphatidic acid: Relevance to tumor growth and angiogenesis. Int J Mol Med 2003;12:633–641.
35. Murph MM, Hurst-Kennedy J, Newton V, Brindley DN, Radhakrishna H. Lysophosphatidic acid decreases the nuclear localization and cellular abundance of the p53 tumor suppressor in A549 lung carcinoma cells. Mol Cancer Res 2007;5:1201–1211.
36. Xie Y, Meier KE. Lysophospholipase D and its role in LPA production. Cell Signal 2004;16:975–981.
37. Fourcade O, Simon MF, Viode C, et al. Secretory phospholipase A2 generates the novel lipid mediator lysophosphatidic acid in membrane microvesicles shed from activated cells. Cell 1995;80:919–927.
38. Rae JM, Creighton CJ, Meck JM, Haddad BR, Johnson MD. MDA-MB-435 cells are derived from M14 melanoma cells—A loss for breast cancer, but a boon for melanoma research. Breast Cancer Res Treat 2007;104:13–19.
39. Cui P, Tomsig JL, McCalmont WF, et al. Synthesis and biological evaluation of phosphonate derivatives as autotaxin (ATX) inhibitors. Bioorg Med Chem Lett 2007;17: 1634–1640.
40. Ferry G, Moulharat N, Pradère J-P, et al. S32826: A nonomolar inhibitor of autotaxin. Discovery, synthesis and applications as a pharmacological tool. J Pharmacol Expt Therap 2008; 327:809–819.
41. Laemmli UK. Cleavage of structural proteins during the assembly of the head of bacteriophage T4. Nature 1970;227: 680–685.
42. Ferguson CG, Bigman CS, Richardson RD, van Meeteren LA, Moolenaar WH, Prestwich GD. Fluorogenic phospholipid substrate to detect lysophospholipase D/autotaxin activity. Org Lett 2006;8:2023–2026.
43. Lee S, Lynch KR. Brown recluse spider (Loxosceles reclusa) venom phospholipase D (PLD) generates lysophosphatidic acid (LPA). Biochem J 2005;391:317–323.
44. Seuwen K, Ludwig MG, Wolf RM. Receptors for protons or lipid messengers or both? J Recept Signal Transduct Res 2006;26:599–610.
45. Murakami N, Yokomizo T, Okuno T, Shimizu T. G2A is a proton-sensing G-protein-coupled receptor antagonized by lysophosphatidylcholine. J Biol Chem 2004;279:42484–42491.
46. Saunders LP, Ouellette A, Bandle R, et al. Identification of small-molecule inhibitors of autotaxin that inhibit melanoma cell migration and invasion. Mol Cancer Ther 2008;7:3352–3362.
47. Samadi N, Gaetano C, Goping IS, Brindley DN. Autotaxin protects MCF-7 breast cancer and MDA-MB-435 melanoma cells against Taxol-induced apoptosis. Oncogene 2008; [Epub ahead of print].